

## RAPID FORMATION OF MOLECULAR CLOUDS AND STARS IN THE SOLAR NEIGHBORHOOD

LEE HARTMANN,<sup>1</sup> JAVIER BALLESTEROS-PAREDES,<sup>2,3</sup> AND EDWIN A. BERGIN<sup>1</sup>

*Received 2001 May 16; accepted 2001 August 2*

### ABSTRACT

We show how molecular clouds in the solar neighborhood might be formed and produce stars rapidly enough to explain stellar population ages, building on results from numerical simulations of the turbulent interstellar medium and general considerations of molecular gas formation. Observations of both star-forming regions and young, gas-free stellar associations indicate that most nearby molecular clouds form stars only over a short time span before dispersal; large-scale flows in the diffuse interstellar medium have the potential for forming clouds sufficiently rapidly and for producing stellar populations with ages much less than the lateral crossing times of their host molecular clouds. We identify four important factors for understanding rapid star formation and short cloud lifetimes. First, much of the accumulation and dispersal of clouds near the solar circle might occur in the atomic phase; only the high-density portion of a cloud's life cycle is spent in the molecular phase, thus helping to limit molecular cloud "lifetimes." Second, once a cloud achieves a high enough column density to form H<sub>2</sub> and CO, gravitational forces become larger than typical interstellar pressure forces; thus, star formation can follow rapidly upon molecular gas formation and turbulent dissipation in limited areas of each cloud complex. Third, typical magnetic fields are not strong enough to prevent rapid cloud formation and gravitational collapse. Fourth, rapid dispersal of gas by newly formed stars, passing shock waves, and reduction of shielding by a small expansion of the cloud after the first events of star formation might limit the length of the star formation epoch and the lifetime of a cloud in its molecular state. This picture emphasizes the importance of large-scale boundary conditions for understanding molecular cloud formation and implies that star formation is a highly dynamic, rather than quasi-static, process and that the low Galactic star formation rate is due to low efficiency rather than slowed collapse in local regions.

*Subject headings:* circumstellar matter — ISM: clouds — stars: formation — stars: pre-main-sequence

### 1. INTRODUCTION

This paper has its origin in the long effort to answer the following deceptively simple question: where are the "post-T Tauri stars" (PTTSs) in the Taurus molecular clouds? As originally suggested by Herbig (1978), there was every reason to expect that the stellar population of Taurus would exhibit a substantial spread in ages, especially if molecular cloud complexes last for several tens of megayears (Elmegreen 1991), and if ambipolar diffusion of magnetic flux over 5–10 Myr is necessary before molecular cloud cores can collapse to form stars (Mouschovias 1991; Shu, Adams, & Lizano 1987). Yet several surveys, beginning with Herbig, Vrba, & Rydgren (1986), found no evidence for a substantial population of PTTSs with ages greater than 3 Myr (Hartmann et al. 1991; Gomez et al. 1992; Briceño et al. 1997, 1999). X-ray surveys of the area did find older stars (Walter et al. 1988; Neuhäuser et al. 1995; Wichmann et al. 1996), but these stars are too dispersed spatially and are too old (~10–100 Myr) to constitute the "missing" greater than 5 Myr old PTTSs of the Taurus clouds (Briceño et al. 1997; Feigelson 1996; see § 2.1).

Taurus is not exceptional. Most star-forming regions containing molecular gas have populations with typical ages ~1–3 Myr, and very few (if any) stars of greater age (see the recent analysis by Palla & Stahler 2000; see also

Hartmann 2001). Moreover, of the substantial molecular cloud complexes within about 350 pc (Taurus, Ophiuchus, Chamaeleon, Corona Australis, Lupus, Serpens, and Perseus), only one, the Coalsack, exhibits little or no evidence for young stars (Nyman 1991; but see Eaton et al. 1990); this indicates that star formation follows the formation of a typical molecular cloud complex within less than 1 Myr (§ 2.1). The age dispersion of stars in clusters suggests that molecular cloud complexes have lifetimes of the order of their dynamical timescales (Elmegreen 2000). Moreover, the absence of ~5–10 Myr old stars in star-forming regions suggests that molecular cloud complexes in the solar neighborhood must coalesce rapidly, form stars rapidly, and disperse rapidly (Hartmann 2000). The view that molecular clouds are relatively transient features goes back at least to the seminal paper by Larson (1981); advances in characterizing the young stellar populations of molecular clouds over the last 20 years reinforce this conclusion.

Rapid cloud evolution has important consequences for understanding the physics of molecular clouds and star formation. If cloud lifetimes are short, there is no need for maintaining a quasi-equilibrium in molecular clouds, so that MHD turbulence (which decays rapidly; Stone, Ostriker, & Gammie 1998; Mac Low et al. 1998; Mac Low 1999) need not be regenerated (Ballesteros-Paredes, Hartmann, & Vázquez-Semadeni 1999a, hereafter BHV99; Elmegreen 2000). Indeed, the limitations placed on cloud lifetimes by stellar populations essentially ensure that the evolution from dispersed molecular gas to protostellar cores is dynamic rather than quasi-static (Ballesteros-Paredes, Vázquez-Semadeni, & Scalo 1999b, hereafter BVS99; Klessen, Heitsch, & Mac Low 2000; Padoan et al. 2001). The low Galactic rate of star formation must be the

<sup>1</sup> Harvard-Smithsonian Center for Astrophysics, 60 Garden Street, Cambridge, MA 02138; hartmann@cfa.harvard.edu, ebergin@cfa.harvard.edu.

<sup>2</sup> American Museum of Natural History, 79th Street at Central Park West, New York, NY 10024; javierbp@amnh.org.

<sup>3</sup> Universidad Nacional Autónoma de México, Instituto de Astronomía, Apdo Postal 70-264, Cd. Universitaria, 04510 México DF, México.

result of reduced efficiency in conversion of gas to stars (Hartmann 1998; Elmegreen 2000) rather than slowing collapse by strong magnetic support.

Solving the post-T Tauri problem by making cloud lifetimes short, however, raises a new set of questions: how are molecular clouds formed so rapidly, and why is it that the clouds form stars so readily, especially given the potential restraining effects of magnetic fields? We argue that formation of clouds and triggering of star formation by large-scale flows, as we argued previously for Taurus (BHV99; see also Sasao 1973; Elmegreen 1993b; Scalo & Chappell 1999), are essential to forming clouds and stars on less than a lateral crossing time. We further show that the conditions needed for molecular gas formation from atomic flows (a minimum column density for shielding and limited turbulent and magnetic support to achieve high enough densities for reasonably rapid chemical evolution) are similar to the conditions needed for gravitational instability (see, e.g., Franco & Cox 1986), with collapse times of order 1 Myr; therefore, star formation can commence rapidly once molecular clouds are produced. We also use general arguments and the results of numerical simulations of the interstellar medium to show that molecular clouds are probably supercritical, and thus magnetic fields do not significantly slow gravitational collapse.

The organization of this paper is as follows. In § 2 we summarize observational constraints from stellar population ages on cloud and star formation timescales. In § 3 we outline a physical scenario in agreement with observations, presenting some numerical results that help support this picture. We consider some further implications of rapid cloud and star formation in § 4, and in § 5 we summarize our conclusions.

## 2. STELLAR POPULATION CONSTRAINTS

### 2.1. Stellar Ages in Associations

The absence of many stars in Taurus and other star-forming regions older than about 3–5 Myr was discussed in detail in BHV99. In view of the importance of the result and the implications of this best-studied cloud for the interpretation of observations of more distant regions, we revisit this issue. We also incorporate updated pre-main-sequence (PMS) stellar isochrones. As discussed, for example, in Hartmann (2001), the principal systematic error in ages for most TTs is uncertainty in the stellar mass. Recent measurements of T Tauri masses using disk rotation (Simon, Dutrey, & Guilloteau 2000) suggest that earlier isochrones underestimated the stellar masses and ages; the net effect of the new estimates, which we use here, is to make the low-mass stars approximately a factor of 2 older than one would infer using the D’Antona & Mazzitelli (1994) tracks as in BHV99.

We begin by focusing on the issue of X-ray-detected stars in Taurus. Neuhäuser et al. (1995) and Wichmann et al. (1996) identified a number of potential PMS stars in the general direction of Taurus from the *ROSAT* All-Sky Survey (RASS) and suggested that these objects represent a significant, older population of Taurus. However, Briceño et al. (1997) pointed out that the mere presence of Li absorption was not a certain indicator of PMS stars, since Li is not strongly depleted in G and early K stars until ages greater than  $\sim 100$  Myr. Moreover, Briceño et al. (1997) showed that *ROSAT* was almost equally sensitive to 100

Myr old stars as to 1–10 Myr old stars, thus the *ROSAT* survey must include many stars much older than 10 Myr. In addition, the observed number of *ROSAT* stellar sources agrees with the number expected for an average formation rate in the solar neighborhood over a 100 Myr period. Briceño et al. (1997) thus argued that most of the *ROSAT* sources are much older than Taurus and thus originated in different clouds that no longer exist. These stars then would disperse considerably over many tens of megayears, thus explaining their smooth spatial distribution and lack of concentration near Taurus. This point of view was supported by Martín & Magazzù (1999), who conducted a careful analysis of Li equivalent widths and concluded that only about 22% of the RASS stars are probably PMS stars.

In a follow-up detailed study, Wichmann et al. (2000) examined 58 of the 72 RASS weak-emission stars with Li found near Taurus and argued that approximately 60% of these were true PMS objects, somewhat higher than the proportion estimated by Martín & Magazzù (1999). However, it is important to place these objects in the appropriate context to understand their significance. To do this, consider Figure 1, where we place these objects in the  $V$  versus  $V-I$  color-magnitude diagram for that portion of the sample (about half) for which Wichmann et al. (2000) present photometry. We also plot isochrones from Siess, Dufour, & Forestini (2000), which are in better agreement with the recent T Tauri mass measurements from disk rotation and agree fairly well with the Palla & Stahler (2000) results.

The most important result to note from Figure 1 is that most of the RASS PMS stars are much older than 10 Myr, assuming that they are at the distance of Taurus. Therefore,

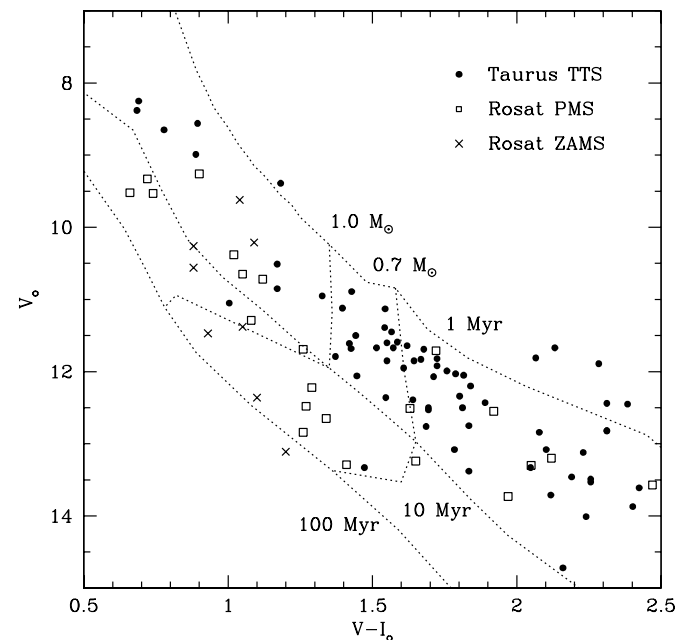


FIG. 1.—Color-magnitude diagram comparing known young TTs with RASS sources. The Taurus colors and extinction corrections have been taken from Kenyon & Hartmann (1995); the *ROSAT* source data have been taken from Wichmann et al. (2000), as discussed in the text. Isochrones and tracks are from Siess et al. (2000). The *ROSAT* sources are not numerous enough to represent a significant star formation epoch in comparison with Taurus; moreover, their substantially greater ages and wide spatial distribution imply that they have mostly formed in widely dispersed clouds that no longer exist (see text).

they cannot explain the drop in star formation rate beyond 3–4 Myr found by Kenyon & Hartmann (1990), BHV99, Palla & Stahler (2000), and Hartmann (2001). Indeed, because there are significantly fewer RASS stars than TTSs in the same mass range, these objects cannot represent a significant local star formation rate. At a constant rate of star formation, there should be  $\sim 10$  times as many 30 Myr old stars as 3 Myr old stars, and this is far from the case, even considering that only about half of the possible RASS sources have photometry and thus are plotted in Figure 1 (a substantial number of TTSs also lack  $V-I$  colors and thus are missing as well). This essential point concerning the star formation rate in Taurus and many other regions has been emphasized strongly by Palla & Stahler (2000).

One should also note that the ages suggested by placement of RASS sources in the color-magnitude diagram are likely to be lower limits. The isochrones assume a distance of 140 pc, and any foreground stars will appear to be too young (the RASS is biased toward foreground stars; Briceño et al. 1997). This possibility is further strengthened by considering the RASS zero-age main-sequence (ZAMS) sources, defined by Wichmann et al. (2000) based on their Li equivalent widths. These stars (Fig. 1, crosses) generally lie well above the main sequence for a distance of 140 pc because they are actually much closer than 140 pc. It would be surprising if the high-Li star sample, selected by the same X-ray criteria, did not have the same bias.

Therefore, we must conclude that the majority of the RASS sources do not belong to the present Taurus molecular cloud complex but must have originated in a much larger area from clouds that no longer exist, as, for example, those that constituted the Gould Belt (Wichmann et al. 2000).

While Taurus is by far the best-studied star-forming region for the purpose of searching for older populations, studies of all other nearby regions yield the same result. Table 1 is a compilation of results from the literature, demonstrating that stellar populations lying within molecular clouds have average ages no larger than about 3 Myr; the molecular gas has been dispersed in some way from

older regions. While one can find small numbers of “older” stars in all these regions, the results of Palla & Stahler (2000) show that these do not imply significant star formation rates. Moreover, as emphasized by Hartmann (2001), the errors in placing stars in the H-R or color-magnitude diagrams are sufficiently large that one should expect to find a few objects with spuriously large ages. Finally, as illustrated in Figure 1, it is extremely easy to contaminate a PMS sample with older foreground populations that did not originate from presently existing molecular gas.

All these considerations reinforce the inference of rapid star formation over limited age spans in molecular clouds. Furthermore, the lack of substantial aggregations of molecular gas without star formation (the Coalsack seems to be the only local exception) indicates that star formation must ensue rapidly upon cloud formation. These time limits place severe constraints on understanding cloud and star formation.

## 2.2. The Crossing Time Problem and Large-Scale Flows

The observational result that poses the greatest challenge to theory is that both the inferred delay time between cloud formation and star formation and the ages of the young stars present can be considerably smaller than the lateral crossing time or dynamical time of the star formation region, suggesting that some kind of external “triggering” must be involved.

For instance, consider the Taurus molecular cloud complex. The projected extent of the Taurus clouds is between  $\sim 20$  and 40 pc (Fig. 2), depending upon whether all the outlying regions of molecular gas are considered to be part of the complex. With a typical velocity dispersion of  $\sim 2 \text{ km s}^{-1}$ , as determined from either the molecular gas motions (e.g., Kleiner & Dickman 1985) or the velocity dispersion of the stellar population (Jones & Herbig 1979), the

TABLE 1  
STAR-FORMING REGIONS

Region	$\langle t \rangle^a$ (Myr)	Molecular Gas?	Ref. (age)
Coalsack .....	...	Yes	...
Orion Nebula .....	1	Yes	1
Taurus .....	2	Yes	1, 2, 3
Oph .....	1	Yes	1
Cha I, II .....	2	Yes	1
Lupus .....	2	Yes	1
MBM 12A .....	2	Yes	4
IC 348 .....	1–3	Yes	1, 4, 5, 6
NGC 2264 .....	3	Yes	1
Upper Sco .....	2–5	No	1, 6, 7
Sco OB2 .....	5–15	No	8
TWA .....	$\sim 10$	No	9
$\eta$ Cha .....	$\sim 10$	No	10

<sup>a</sup> Average age in Myr.

REFERENCES.—(1) Palla & Stahler 2000. (2) Hartmann 2001. (3) White & Ghez 2001. (4) Luhman 2001. (5) Herbig 1998. (6) Preibisch & Zinnecker 1999. (7) Preibisch et al. 2001. (8) de Geus et al. 1989. (9) Webb et al. 1999. (10) Mamajek, Lawson, & Feigelson 1999.

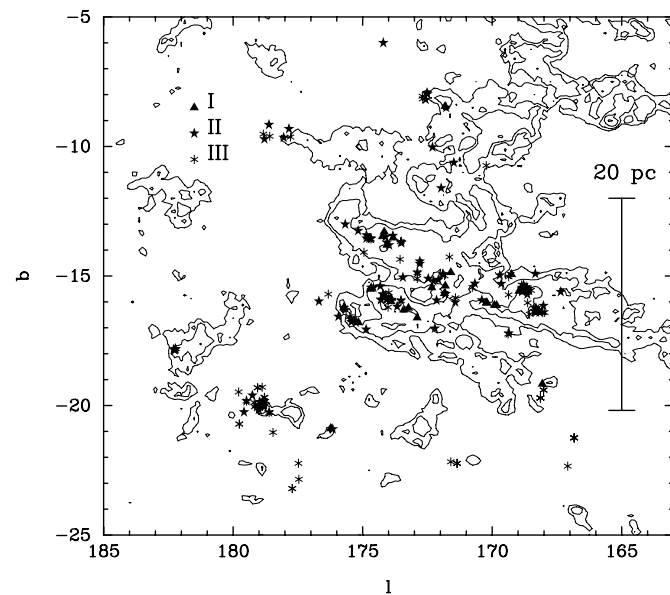


FIG. 2.—Distribution of young stars in the Taurus molecular cloud, superimposed upon  $^{12}\text{CO}$  emission contours taken from T. Megeath, T. Dame, & P. Thaddeus (2001, in preparation; see Dame et al. 2001). Class I, II, and III sources are indicated, corresponding to protostars, stars with disks, and stars without disks, respectively. The majority of the stars in this plot have ages  $\sim 2$  Myr and an age spread not more than 2–4 Myr, even though the lateral extent of the region approaches 40 pc and thus the associated crossing time is of order 20 Myr (see text).

lateral crossing time of the Taurus complex is then 10–20 Myr. Yet, using the most up-to-date calibrations of stellar evolutionary tracks (e.g., Simon et al. 2000), the average age of the stars in Taurus is only about 2 Myr, and the ages of the vast majority of the stars are less than  $\sim 4$  Myr (Palla & Stahler 2000; Hartmann 2001; White & Ghez 2001).

While the youth of stars in molecular clouds has been recognized as a problem for standard theories of low-mass star formation (e.g., Hartmann et al. 1991; Feigelson 1996; Briceño et al. 1997; Palla & Galli 1997), the constraints posed by gas-free but relatively youthful stellar associations have been underappreciated. Consider the Sco OB2 association, which consists of three subgroups spanning a total length of  $\sim 150$  pc (Blaauw 1960, 1964, 1991; de Zeeuw et al. 1999; de Bruijne 1999). Assuming that the (one-dimensional) stellar velocity dispersion of only  $\lesssim 1.5$  km s $^{-1}$  found by de Bruijne (1999) from an analysis of *Hipparcos* data is representative of the motions in the parent molecular cloud that formed Sco OB2 (as in Taurus; see above paragraph), the lateral crossing time of the entire complex is  $\sim 150$  Myr.<sup>4</sup> However, the ages of the Sco OB2 subgroups span a range of only 10 Myr (de Geus, de Zeeuw, & Lub 1989; Preibisch & Zinnecker 1999; Preibisch, Günther, & Zinnecker 2001), or about 15 Myr if one includes the  $\sim 1$  Myr old Ophiuchus molecular cloud complex at one end of the association.

The obvious conclusion to be drawn is that the lateral crossing times of elongated star-forming regions are (often) irrelevant to formation processes. What is required is some mechanism of triggering the onset of cloud and star formation that operates externally, spans large scales, and does not require the propagation of information laterally to trigger star formation.

<sup>4</sup> Mamajek, Lawson, & Feigelson (2000) suggest that the Sco OB2 subgroups may have been somewhat closer together ( $\sim 100$  pc span) about 10 Myr ago, but J. H. J. de Bruijne (2001, private communication) finds that the proper motions of the subgroups are the same within the observational errors. In any case this reduction in the initial size of the association still requires a propagation speed for any external trigger of 7–10 km s $^{-1}$  along the long dimension, still much larger than the observed stellar velocity dispersion.

Recently some of us (BHV99) presented observational evidence and theoretical arguments suggesting that the Taurus molecular cloud complex (and by inference, many other star-forming regions) could have been formed very rapidly by converging supersonic large-scale flows powered by the global energy input from previous episodes of star formation. The importance of large-scale turbulence and flows has previously been emphasized by Sasao (1973), Elmegreen (1993b), and Scalo & Chappell (1999). In this picture, molecular clouds are formed in the postshock gas with a lateral extent set by the coherence in the large-scale velocity field; then the relevant crossing or dynamical time is that of the shortest dimension, not the longest.

While the idea that cloud and star formation can be triggered by flows driven by massive stars is hardly new (e.g., Blaauw 1964, 1991; Elmegreen & Lada 1977; McCray & Kafatos 1987), this picture (see also Vázquez-Semadeni, Passot, & Pouquet 1995) differs from some other scenarios by recognizing that stellar energy input can drive flows over very large scales, i.e., hundreds of parsecs, as in the “supershell” picture of McCray & Kafatos (1987). In this picture, the global stellar energy input feeds the turbulence at small scales, but local bubbles expand and interact with their surrounding medium such that the morphology of the structures can become complicated (and in general do not exhibit simple bubble geometry).

The large-scale nature of the flow field has several important consequences. Large-scale motions make it much easier to form extremely large structures in which star formation can be triggered nearly simultaneously. The simplest example of this is a shell driven outward by winds and supernovae (SNe) from massive stars in a central cluster (Fig. 3, *left panel*). The expanding shell eventually sweeps up enough mass to become gravitationally unstable and form stars. If the radius of the shell or bubble is large enough, star formation can be coordinated over very large distances, as a result of having a common event driving evolution in the radial direction, rather than any propagation of compression along the shell. An example of this type of structure may be found in the Cep OB2 association (Patel et al. 1995, 1998).

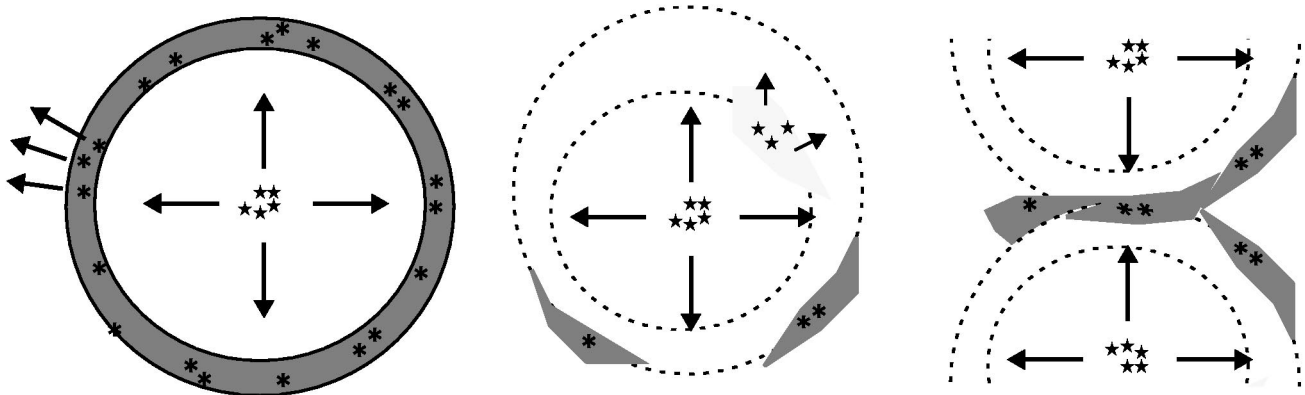


FIG. 3.—Schematic view of large-scale triggered star formation. In the simplest possible case (*left*), star formation produces an expanding shell that eventually becomes self-gravitating. Densities in the swept-up shell may therefore achieve similar values over very large scales, and thus star formation can be coordinated over timescales much shorter than the lateral crossing time (the bubble radius divided by the velocity dispersion of the shell). The velocity dispersion among the stars formed in this gas can be small, much less than the overall expansion velocity of the shell, over regions small in comparison with the shell radius. Because the ISM is unlikely to be uniform on large scales, the shell density will not be uniform, and so star formation cannot be simultaneous over the entire shell (*center*), implying a range of star formation epochs. However, if clouds are rapidly dispersed by the star-forming event, the lifetime of molecular gas in any particular region can still be short. In general, the large-scale numerical simulations of the ISM by PVP95, BHV99, etc., suggest that most clouds will be formed from the interactions of flows from distinct star-forming sites (*right*).

A second consequence of the large-scale nature of the motions in the interstellar medium (ISM) is that flows driven by different regions interact to form complex structures that in general are not simply related to specific triggering sites (Figure 3, *right panel*). Thus, the Taurus complex may have been triggered by interacting flows even though it looks nothing like a ring or shell (Fig. 2).

In contrast to triggering by nonlocal flows, local triggering models appear to have some difficulties in explaining spatially extended associations with small velocity dispersions like Taurus and Sco OB2. Propagation speeds of  $10\text{--}15\text{ km s}^{-1}$  are needed to trigger star formation across these regions within the required age spans. It is clear that the molecular gas that is forming stars in Taurus, or has formed stars in Sco OB2, cannot have been moving this fast; there is no evidence for such velocity dispersions and gradients from the stellar proper motions in Taurus and Sco OB2 (Jones & Herbig 1979; de Bruijne 1999). Therefore, the models of Blaauw (1964, 1991), Elmegreen & Lada (1977), de Geus et al. (1989), and Preibisch & Zinnecker (1999) for Sco OB2 require that the large-scale molecular cloud must have existed long before the local triggering by stellar energy input occurred. In other words, in local triggering models the cloud formation process is independent of the star formation process. However, these models further demand no significant star formation in the extended molecular cloud, over a period of 5–10 Myr prior to triggering; otherwise, triggering would not be needed, and a large spread in stellar ages would result, which is not observed in the youngest group, Upper Sco (Preibisch & Zinnecker 1999). The evidence of Table 1 suggests that it is unlikely that such large masses of molecular gas would have remained inert for such a long time. The nonlocal flow picture avoids this problem by making the triggering of cloud formation the same event as the triggering of star formation.

Putting it another way, one clear indication of triggering cloud and star formation would be to see swept-up, moving gas producing stars. The small dispersion in stellar proper motions in Sco OB2 provides little evidence that swept-up gas driven by the oldest stars (Upper Cen–Lupus) was decisive in producing star formation in the younger Upper Sco–Oph regions. These issues should be addressed further with hydrodynamic simulations.

In summary, while driving from local star formation may help trigger new star formation locally, large-scale structures with small velocity dispersions and young stellar populations generally require large-scale, external triggering.

### 3. RAPID FORMATION OF MOLECULAR CLOUDS AND STARS

The simulations shown by BHV99 suggest that clouds in the ISM may be formed “rapidly” by large-scale flows. Specifically, BHV99 showed that the flows could produce clouds that evolve to high densities over scales of tens of parsecs nearly simultaneously (i.e., within a few megayears). These simulations did not follow molecular gas formation or demonstrate gravitational collapse because they were limited to densities less than  $100\text{ cm}^{-2}$ . As most of the gas at the solar circle is in diffuse H I, it is necessary to consider the transformation between atomic and molecular gas. A more complete picture can be developed by augmenting the results of simulations with some additional physical con-

siderations, as described below. In this section we focus on conditions particularly relevant to low-density star-forming regions in the solar neighborhood.

#### 3.1. Cloud Accumulation and Molecular Gas Shielding

Even with the typical ISM flow velocities  $\sim 10\text{ km s}^{-1}$  found by BHV99, it can take tens of megayears to accumulate enough mass from the diffuse ISM to form a molecular cloud complex (§ 4). However, a necessary (though not sufficient) condition for the existence of molecular material in the solar neighborhood is that it have a large enough column density to effectively shield  $\text{H}_2$  and CO from the dissociating ultraviolet radiation of the diffuse Galactic field. This requires a minimum column density in hydrogen atoms of roughly (van Dishoeck & Black 1988; van Dishoeck & Blake 1998)

$$N_{\text{H}}(\text{min}) \approx 1\text{--}2 \times 10^{21}\text{ cm}^{-2}, \quad (1)$$

or

$$A_{\text{V}}(\text{min}) \approx 0.5\text{--}1. \quad (2)$$

Thus, even if the process of building up material from diffuse H I takes a long time, the relevant lifetime for the molecular cloud (or a dark cloud) at the solar circle only begins once this minimum column density is attained. A substantial portion (in some cases the majority) of the time spent in adding mass to an eventual molecular cloud may not contribute to the molecular cloud “lifetime.” Since it is much more difficult to detect concentrations of atomic hydrogen in the Galactic plane than it is to find molecular clouds, any possible pre-molecular state of the cloud would be essentially “invisible.” (See, for example, Fig. 2 of BHV99, which illustrates the difficulty of finding atomic gas associated with Taurus, even at its high Galactic latitude.)

Conversely, disrupting the molecular cloud may not always require physically moving the gas large distances. Instead, simply expanding the cloud material to the point where the column density falls below the critical value of  $N_{\text{H}}(\text{min})$  for self-shielding could be sufficient, especially in low-density regions. We return to the question of dispersal mechanisms in § 5.

Dame (1993) estimated that the ratio of H I to  $\text{H}_2$  within about 1 kpc of the Sun is about 4:1. If we assume that this ratio represents the average relative timescales for molecular and atomic phases, and if molecular regions last for 3–5 Myr as suggested by Table 1, the atomic phase between cloud formation epochs might last  $\sim 12\text{--}20$  Myr, which is consistent with a substantial accumulation period as atomic gas (at the solar circle).

#### 3.2. Molecular Gas Formation

Rapid formation of molecular gas also requires a minimum density as well as shielding. We will present detailed calculations of the physical and chemical post-shock evolution of gas produced by colliding flows in the diffuse neutral atomic medium in a subsequent paper (E. Bergin et al. 2001, in preparation). For present purposes we can constrain parameters as follows. For atomic hydrogen densities greater than about  $n_{\text{H}} \sim 10^2\text{ cm}^{-3}$  and pressures  $(P/k)_4 \gtrsim 1$  [where  $(P/k)_4$  is measured in units of  $10^4\text{ cm}^{-3}\text{ K}$ ], the heating and cooling rates in an unshielded atomic medium are sufficiently fast to approach temperature equilibrium in  $\lesssim 10^5$  yr, which is essentially instantaneous for our purposes (see Wolfire et al. 1995,

their eq. [10], and associated discussion). We may then use the equilibrium results of Wolfire et al. (1995) to estimate the temperature and density of the postshock cooling layer prior to the time at which shielding by dust (and self-shielding by  $\text{H}_2$ ) becomes important. For pressures  $(P/k)_4 \gtrsim 1$ , the temperature approaches values  $\sim 30$  K for densities  $\gtrsim 300 \text{ cm}^{-3}$ . Because the temperature will decline further once shielding becomes important, and cosmic-ray heating will tend to maintain a minimum gas temperature  $T \gtrsim 10$  K, we expect relevant gas temperatures to lie in the range 10–30 K.

The dust temperature may also be an important factor in  $\text{H}_2$  formation. Tielens & Allamandola (1987) show that the evaporation time of the H atom from a grain becomes shorter than the timescale for an H atom to scan a grain surface at temperatures  $\gtrsim 30$  K. The exact temperature dependence is uncertain as it will depend on various grain properties and on whether the grain itself is coated by a layer of water molecules. Some detailed calculations by J. Black (2001, private communication) suggest that grain temperatures must be  $T \lesssim 15$  K in order for  $\text{H}_2$  formation to proceed rapidly. Dust temperatures in the diffuse (unshielded) ISM are uncertain; observational estimates range from about 13 to 22 K (Lagache et al. 1998; Wright et al. 1991; Sodroski et al. 1997).

Some small amount of extinction therefore may be required to lower grain temperatures such that H atoms remain on the surface long enough to locate another H atom and react. Burton, Hollenbach, & Tielens (1990) find that, for standard interstellar radiation fields, the dust temperature should scale roughly as

$$T \propto \left[ \exp \left( - \frac{1.8A_V}{1.086} \right) \right]^{0.2}. \quad (3)$$

If the unshielded dust temperature is  $\sim 20$  K, then shielding of  $A_V \sim 0.8$  would reduce the dust temperature to  $\sim 15$  K. Thus, it seems reasonable to assume that in the shielded postshock layer, dust temperatures will be low enough for efficient  $\text{H}_2$  formation.

With this assumption, we can estimate the  $\text{H}_2$  formation rate. If we adopt the formula of Hollenbach, Werner, & Salpeter (1971),

$$R_{\text{HWS}} = 2.25 \times 10^{-18} T^{1/2} y_f \text{ cm}^{-3} \text{ s}^{-1}, \quad (4)$$

where  $T$  is the gas temperature, and assume a sticking fraction  $y_f = 0.3$ , the formation timescale is

$$t_{\text{HWS}} \sim (R_{\text{HWS}} n_{\text{H}})^{-1} \\ \sim 15 n_3^{-1} T_{10}^{-1/2} \text{ Myr} = 15 \left[ \left( \frac{P}{k} \right)_4 \right]^{-1} T_{10}^{1/2} \text{ Myr}, \quad (5)$$

where  $n_3$  is the hydrogen density in units of  $10^3 \text{ cm}^{-3}$  and  $T_{30}$  is the temperature in units of 30 K. This timescale is long compared to the timescales implied by stellar population ages in molecular clouds, especially for pressures comparable to the typical galactic pressure  $(P/k)_4 \sim 1$  (Mathis 2000; see estimates summarized by Norman 1995). However, other sources yield differing rates. For example, the observational results of Jura (1975) suggested net rates of formation approximately a factor of 3–10 higher than implied by equation (4). Similarly, the rates of Tielens & Hollenbach (1985), which were used by Koyama & Inutsuka (2000) to study  $\text{H}_2$  formation in an unshielded

postshock gas, would yield timescales about a factor of 3 shorter,

$$t_{\text{TH}} \sim 5 n_3^{-1} T_{10}^{-1/2} \text{ Myr} = 5 \left[ \left( \frac{P}{k} \right)_4 \right]^{-1} T_{10}^{1/2} \text{ Myr} \quad (6)$$

(equivalent to setting  $y_f \sim 1$  in eq. [4]).

It may be that cloud formation in the solar neighborhood is mainly driven by pressure forces a few times larger than the average pressure, so that  $\text{H}_2$  formation is more rapid. In addition, as we show in the next section, once a shielding column density is attained, gravitational forces start to become important, which will cause the cloud to contract and become denser; factors of a few increase in density would be sufficient to ensure rapid molecular gas formation. Turbulent and clumpy internal structure (Elmegreen 2000) may also play a role in elevating local densities and thus help form molecules.

We will present a detailed analysis of molecular gas formation in a subsequent paper (E. Bergin et al. 2001, in preparation). For the present, it appears to be possible to form  $\text{H}_2$ , with CO formation following closely thereafter (Bergin, Langer, & Goldsmith 1995), within a few megayears once gas densities reach  $\sim 10^3 \text{ cm}^{-3}$  (see also Koyama & Inutsuka 2000).

### 3.3. Gravitational Instability

The observations imply that soon after molecular clouds are formed, stars are produced. We next show that, under “ideal” circumstances, clouds with sufficient shielding can collapse gravitationally, on a sufficiently short timescale, and then consider limiting factors.

In our picture, the molecular cloud is the postshock region of converging flows. As described in § 3.2, for gas pressures near the fiducial value, the temperature in the postshock region should rapidly decay to values of less than 30 K. An idealization of this situation, which provides the most favorable conditions for gravitational collapse, is an infinite, planar, isothermal, and nearly static layer (since the postshock flow velocity is greatly reduced at high density). For such a layer, the central pressure is (Ledoux 1951; Spitzer 1978; Elmegreen & Elmegreen 1978)

$$P_c = P_e + \frac{\pi G \Sigma^2}{2}, \quad (7)$$

where  $P_e$  is the external pressure and  $\Sigma$  is the total column density through the sheet. Assuming that the cloud is molecular, the internal pressure due to self-gravity is comparable to the external pressure for a column density of hydrogen atoms

$$N_{\text{H}} \sim 1.5 \times 10^{21} \left( \frac{P_e}{k} \right)_4^{1/2} \text{ cm}^{-2}, \quad (8)$$

or

$$A_V \sim 0.8 \left( \frac{P_e}{k} \right)_4^{1/2}. \quad (9)$$

Thus, the column density needed to produce a detectable dark cloud and to allow molecular gas to form (§§ 3.1 and 3.2) is comparable to that required for self-gravity to be important in comparison with external pressure forces (Franco & Cox 1986; Elmegreen 1991). We argue that this coincidence between the column density needed for

molecular shielding and that required for important self-gravitating forces is the basic reason why star formation is presently occurring in virtually all molecular cloud complexes of significant size in the solar neighborhood.

We next investigate the possible scales of gravitational instability and the associated collapse timescales. For an isothermal infinite sheet in hydrostatic equilibrium, neglecting the external pressure, the critical spatial wavenumber for stability is (Ledoux 1951; Spitzer 1978)

$$k_c = \frac{\pi G \Sigma}{c_s^2}, \quad (10)$$

corresponding to a Jeans length

$$\lambda_c \equiv \frac{2\pi}{k_c} = 0.7 T_{10} N_{21}^{-1} \text{ pc}, \quad (11)$$

where we have assumed that the gas is molecular,  $T_{10}$  is the temperature in units of 10 K, and  $N_{21}$  is the molecular hydrogen column density in units of  $10^{21} \text{ cm}^{-2}$ . The maximum growth rate  $\Gamma_{\text{max}}$  occurs on a wavenumber approximately twice critical, or a wavelength  $2\lambda_c$ , and has a value (Simon 1965)

$$\Gamma_{\text{max}} \approx 0.67 \pi G \frac{\Sigma}{c_s} = 3.6 \times 10^{-14} N_{21} T_{10}^{-1/2} \text{ s}^{-1}, \quad (12)$$

for a characteristic growth time

$$\tau_{\text{min}} = \Gamma_{\text{max}}^{-1} \sim 0.9 \times 10^6 T_{10}^{1/2} N_{21}^{-1} \text{ yr}. \quad (13)$$

Linear growth rates remain within a factor of about 2 of the maximum rate  $\Gamma_{\text{max}}$  for wavelengths between  $\sim 1.07\lambda_c$  and  $\sim 15\lambda_c$  (Simon 1965), so the above timescale for collapse is not very sensitive to the scale involved. Thus, once the column density approaches the minimum shielding value and the temperature drops below 30 K, it is possible for molecular gas to collapse gravitationally on timescales of order 1–3 Myr over a wide range of length scales and masses.

The criterion of equation (8) or equation (9) is not a strict guide to the onset of gravitational collapse. In principle, gravitational instability can occur at lower surface densities (e.g., Elmegreen & Elmegreen 1978). However, low surface density clouds are much more susceptible to disruption by external pressures and are more likely to be supported against gravity by turbulent motions. To examine the effects of external pressure distortion, consider an idealized situation in which the flows produce a curved, expanding shell (i.e., Fig. 3). An expanding shell can be stabilized against gravity if (Vishniac 1983)

$$\Gamma_{\text{max}} \ll \frac{V_s}{R_o}, \quad (14)$$

where  $V_s$  is the shell expansion velocity and  $R_o$  is the radius (or characteristic radius of curvature) of the shell. This implies that the above sheet can be prevented from collapsing if the characteristic radius of curvature is

$$R_o \ll 9 \left( \frac{V_s}{10 \text{ km s}^{-1}} \right) T_{10}^{1/2} N_{21}^{-1} \text{ pc}. \quad (15)$$

Because observed cloud structures tend to be much larger than a few parsecs (and tend to be driven over much larger scales than this; § 4), expansion is unlikely to be a general

obstacle to gravitational collapse for column densities near or above the shielding constraint.

Similarly, uniform rotation can also suppress gravitational instability above a critical value of the Toomre  $Q$  parameter

$$Q_c = \frac{c_s \Omega}{\pi G \Sigma} = 0.338 \quad (16)$$

(Goldreich & Lynden-Bell 1965a), where  $\Omega$  is the angular frequency.<sup>5</sup> In terms of a maximum rotational velocity gradient,

$$\Omega_c^{-1} \sim (0.55 \text{ km s}^{-1}) T_{10}^{-1} N_{21} \text{ pc}^{-1}. \quad (17)$$

Again, this does not appear to be a major limitation for column densities near or above the necessary shielding length. For example, the radial velocity gradient across the main component of the Taurus complex is  $\approx 0.25 \text{ km s}^{-1} \text{ pc}^{-1}$  (Kleiner & Dickman 1985), although in some smaller regions the gradients may approach  $1 \text{ km s}^{-1} \text{ pc}^{-1}$  (Arquilla & Goldsmith 1986).

### 3.4. Turbulence

It has been generally accepted since Chandrasekhar & Fermi (1953) that turbulent motions can give rise to internal pressure support, which could prevent cloud and star formation. For example, if the  $\sim 2 \text{ km s}^{-1}$  “turbulent” velocities observed in the Taurus molecular complex corresponded only to extremely small-scale motions, the resulting internal turbulent pressure would prevent the postshock gas from condensing to densities greater than  $15(P/k)_4 \text{ cm}^{-3}$ . This would imply that to form molecular gas, either (1) pressures must be 2 orders of magnitude larger than typical interstellar pressures, (2) turbulent motions damp rapidly, or (3) these motions do not correspond purely, or even mostly, to very small scale turbulence. In fact, Sasao (1973) demonstrated that large-scale turbulence plays an important role as a generator of astronomical objects and that the role of the turbulent pressure might be only of a higher order. Moreover, based on numerical simulations, Léorat, Passot, & Pouquet (1990) and Klessen et al. (2000) have shown that local collapse may be hindered only if turbulence is present at the very smallest scales; in a realistic turbulent medium, turbulence can support the cloud globally while promoting local collapse (Klessen et al. 2000).

We argue that, even in situations where (1) is not appropriate, factors (2) and (3) can result in rapid formation. Recent numerical simulations show that turbulent motions do decay rapidly in molecular clouds, generally on a crossing time for any scale involved (Stone et al. 1998; Mac Low et al. 1998; Padoan & Nordlund 1999), or on timescales smaller than the free-fall timescale (Mac Low 1999). Here the important point is that the relevant distance for the crossing time is the shortest dimension, not the longest. For the fiducial pressure  $(P/k)_4 = 1$  and a temperature of 10 K, the physical length at a column density of  $N_{21} = 2$  is  $\sim \frac{2}{3} \text{ pc}$ , and the crossing time at a turbulent velocity of  $1\text{--}2 \text{ km s}^{-1}$  would therefore be less than 1 Myr.

<sup>5</sup> For differentially rotating regions, shearing perturbations can grow by large factors even when nonshearing perturbations are stable (Goldreich & Lynden-Bell 1965b; Toomre 1981). However, in the case of shear, replacing  $\Omega$  by the epicyclic frequency  $\kappa$  in eqs. (16) and (17) changes the stability criterion only by factors of order unity.

Star-forming molecular clouds do exhibit substantial turbulent velocities of  $\sim 1\text{--}2 \text{ km s}^{-1}$  on size scales of a few parsecs (e.g., Larson 1981), so that not all of the turbulent motions have decayed at the epoch of star formation. However, the internal motions of molecular clouds most likely do not correspond to only very small scale turbulence but instead contain substantial energy on large scales, i.e., diverging and converging flows, as has been suggested based on results of numerical simulations of cloud turbulence by BVS99. These large-scale motions are particularly susceptible to efficient dissipation of energy in shocks. In addition, simulations show that superposition of independent regions along the line of sight cannot be ignored when attempting to interpret observations (Kwan & Sanders 1986; BVS99). For this reason observed turbulent velocities can easily result in an overestimate of internal (small-scale) velocity dispersions, as has been pointed out by Ostriker, Stone, & Gammie (2001), and it is difficult to determine when an observed clump is actually a physical entity or the superposition of different regions along the same line of sight (Ballesteros-Paredes & Mac Low 2001). In other words, individual clumps could have low internal velocity dispersions even though moving supersonically relative to each other along the line of sight (Kwan & Sanders 1986).

Moreover, Ballesteros-Paredes (1999,<sup>6</sup> 2000) has shown that even if there is equipartition between the kinetic, magnetic, and gravitational energy components (Ballesteros-Paredes & Vázquez-Semadeni 1995, 1997), the kinetic energy term (pressure) does not necessarily contribute support against gravity; cloud compression as well as expansion or disruption can result from such turbulence. In examining these possibilities it is important to consider not only the internal motions but also surface forces as well (BVS99). In fact, as has been shown by Klessen & Burkert (2001) and Klessen et al. (2000), large-scale turbulence is able to form dense, elongated structures that will collapse rapidly, producing clustered star-forming regions.

Our picture, then, of a molecular cloud is one in which the small-scale turbulent motions are smaller than frequently estimated because of superposition effects, and which in any event are rapidly damped, allowing the gas to reach high enough densities to form  $\text{H}_2$  and CO rapidly

( $t < 10 \text{ Myr}$ ). It is important to keep in mind that the low efficiency of star formation in most nearby clouds (e.g., Cohen & Kuhi 1979) requires that only a small fraction (generally, a few percent) of the molecular gas collapses to form stars. Thus, damping of turbulence need not be complete in the entire cloud complex for our picture to hold.

### 3.5. Magnetic Fields: Compression and the “Flux Problem”

The pressure from (nonturbulent) magnetic fields potentially could prevent postshock densities from rising to high enough values to form molecular gas rapidly. In ideal MHD, steady one-dimensional flow, the shock relations for the field component  $B_t$  perpendicular to the shock front result in  $B_t \propto \rho$  in the postshock gas (McKee & Hollenbach 1980). Assuming an oblique shock, as illustrated schematically in the left-hand panel of Figure 4, the field thus becomes increasingly parallel to the shock front as the gas cools and becomes denser, eventually limiting the maximum density achieved. The ratio of the maximum postshock density,  $n_m$ , to the initial density,  $n_o$ , is given by (McKee & Hollenbach 1980)

$$\frac{n_m}{n_o} \sim 35 \left( \frac{P_e}{k} \right)_4^{1/2} \frac{B_{o,t}}{1 \mu\text{G}}, \quad (18)$$

where  $B_{o,t}$  is the initial transverse magnetic field strength. Assuming diffuse interstellar gas densities of a few per centimeter cubed, flow velocities of order  $10 \text{ km s}^{-1}$ , and random magnetic field strengths of  $\sim 5 \mu\text{G}$  (Mathis 2000), it would be impossible to achieve the densities of  $10^3 \text{ cm}^{-3}$  needed to form molecular gas rapidly unless the flows are essentially parallel to the magnetic field (so that  $B_{o,t} < 1 \mu\text{G}$ ) (e.g., Hennebelle & Pérault 1999). Unless the magnetic fields are very strong, so that flows are channeled completely along field lines (Passot, Vázquez-Semadeni, & Pouquet 1995, hereafter PVP95; Ostriker, Gammie, & Stone 1999; Ostriker et al. 2001), cloud formation would seem to be a very unlikely event.

However, the numerical simulations of PVP95, Ostriker et al. (1999, 2001), and Heitsch, Mac Low, & Klessen (2001) show that the geometry indicated in Figure 4 and expressed in equation (18) generally is not relevant for understanding cloud formation when the magnetic field is weak or of intermediate strength with respect to the turbulent gas pressure. Unlike the field geometry shown in the left-hand panel of

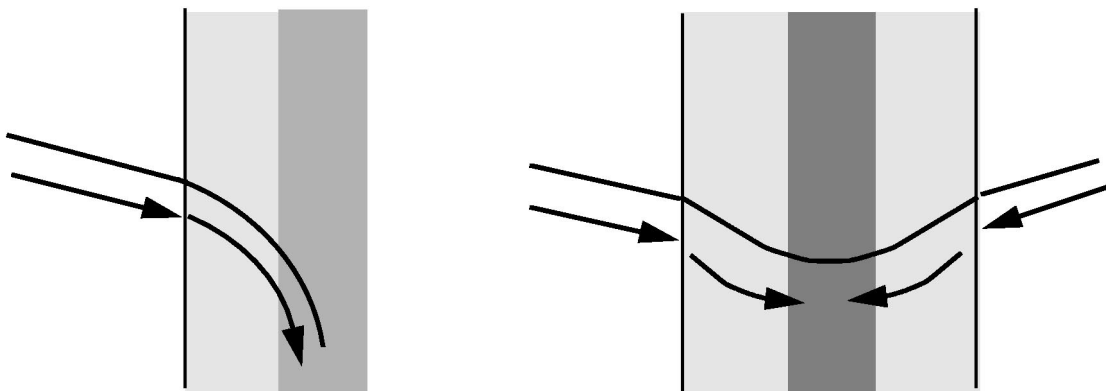


FIG. 4.—*Left panel*: Assumed field geometry for the one-dimensional steady MHD oblique shock model. The field becomes increasingly tangential as the postshock gas cools, resulting in a magnetic pressure that eventually limits compression. *Right panel*: Typical geometry of clouds seen in numerical simulations with magnetic fields in roughly equipartition strength with the turbulent gas pressure. The clouds tend to form in kinks or bends in the field lines, and dense regions in the postshock gas arise preferentially near where the tangential magnetic field becomes small (see text).

<sup>6</sup> <http://research.amnh.org/javierbp>.

Figure 4, clouds tend to form at bends or “kinks” in the magnetic field (Fig. 5; see also BVS99). This means that there are regions in the cloud where  $B_t \rightarrow 0$  (approximately parallel to the major axis of the cloud), and it is here where gas compression can proceed unabated by magnetic forces. Thus, the compression of the parallel magnetic field in such configurations can delay, but cannot ultimately prevent, postshock gas from compressing to high densities as it cools.

A more difficult question is whether the magnetic field component more or less perpendicular to the shock front(s) and the main axis of the cloud is strong enough to delay or suppress gravitational collapse into stars. A very large literature exists that assumes that magnetic fields are initially strong enough to prevent gravitational collapse (e.g., Mouschovias 1991 and references therein), although recent observational results (Crutcher 1999; Jijina, Myers, & Adams 1999; Lee & Myers 1999; Bourke et al. 2001) and theoretical analyses (Nakano 1998; Padoan & Nordlund 1999; Ciolek & Basu 2001) suggest that the effects of magnetic fields in preventing or slowing collapse may be much less than previously thought.

To simplify as much as possible, consider our thin (infinite, isothermal, self-gravitating) sheet from §§ 3.1–3.3, threaded by a perpendicular magnetic field. Gravitational collapse can ensue only if (Nakano & Nakamura 1978)

$$G\Sigma_c^2 > \frac{B^2}{4\pi^2}. \quad (19)$$

Multiplying both sides by the area of the cloud and taking the square root,

$$(4\pi^2 G)^{1/2} M_c > \Phi_B, \quad (20)$$

where  $M_c$  is the cloud mass and  $\Phi_B$  is the magnetic flux threading the cloud. Clouds satisfying equation (19) or equation (20) are said to be magnetically supercritical;

otherwise, the clouds are magnetically subcritical. (In different geometries the numerical relation in eq. [20] changes modestly, without altering the fundamental relation.) If flux freezing holds, a subcritical cloud will never be able to collapse gravitationally. Magnetic flux therefore must be removed from the cloud before stars can form. This cannot occur easily in the diffuse ISM or even in low column density regions of molecular clouds (Myers & Khersonsky 1995) because the magnetic field lines are well coupled to the gas. In this situation, collapse to stars cannot occur until magnetic flux is removed via ambipolar diffusion in the dense, highly shielded cloud regions where the ionization is very low.

In the standard model of low-mass star formation, protostellar clouds can be magnetically subcritical by a wide margin (e.g., Shu et al. 1987; Mouschovias 1991 and references therein). The timescale for the necessary ambipolar diffusion of magnetic flux can be as long as 5–10 Myr, depending upon how subcritical the cloud is initially. But this is inconsistent with the stellar population ages. One would expect a delay of at least several megayears between the time of molecular gas formation and the onset of star formation (Palla & Galli 1997), and this is not observed in the solar neighborhood. In addition, it is implausible that all regions of all clouds are subcritical to the same extent; therefore, there should be spread of diffusion timescales, and thus ages, comparable to the overall diffusion time. This would result in age spreads of 5–10 Myr in the case of very subcritical initial conditions, which again is not observed.

The solution to this dilemma is that molecular clouds must be initially supercritical (Hartmann 1998; Nakano 1998), or at least close to critical so that only a small amount of magnetic flux need be diffused away (e.g., Ciolek & Basu 2001). Reassuringly, observations indicate that molecular clouds are nearly critical or slightly supercritical

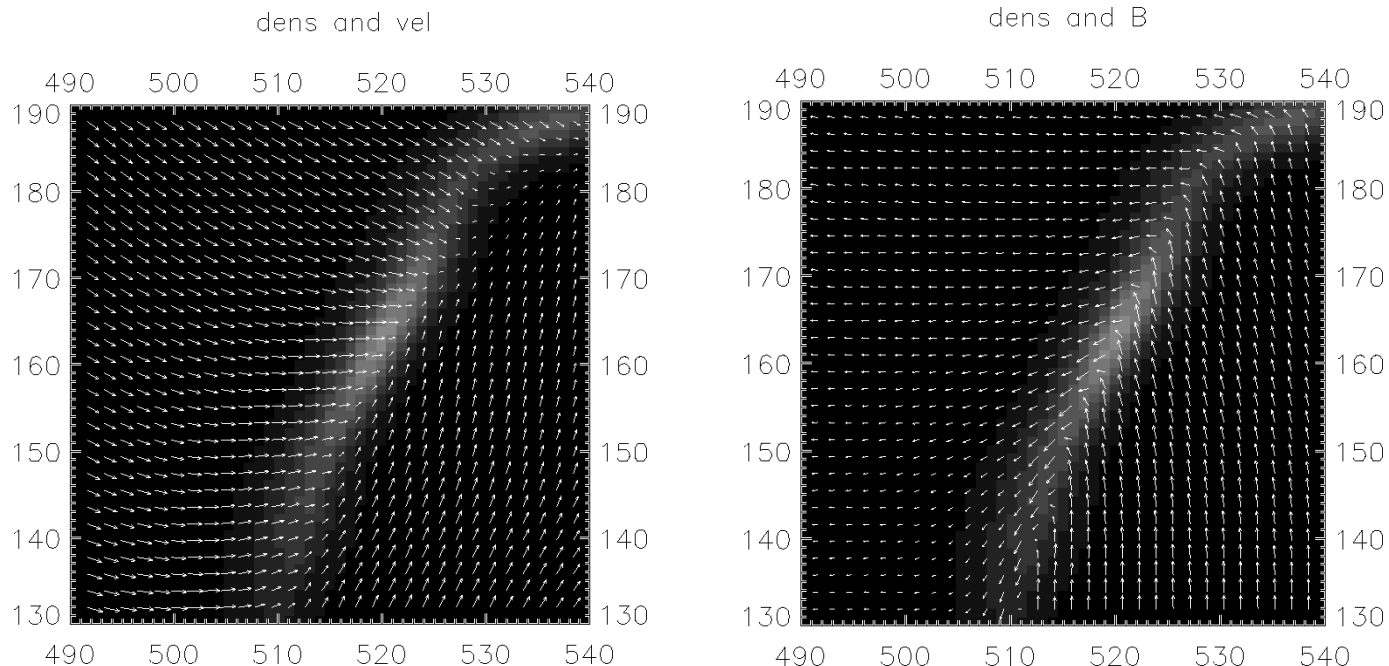


FIG. 5.—Velocity (*left*) and magnetic (*right*) fields superimposed on density gray-scale levels for the cloud discussed in BHV99. The formation of the cloud at a bend or “kink” in the magnetic field is evident.

on large scales (McKee 1989; McKee et al. 1993) and even in denser cloud cores (Crutcher 1999; Bourke et al. 2001).

A clue to why clouds are initially supercritical is given by numerical simulations. Ostriker et al. (2001) noted that condensations can form whether the regions inside their computational region are magnetically subcritical or supercritical, but gravitational collapse ensues only for the supercritical cases. PVP95 also found that gravitational collapse can occur when the computational region (in this case a large section of the Galactic disk in two dimensions) is magnetically supercritical. These results demonstrate the importance of boundary conditions. With periodic boundary conditions (as is the case of the numerical simulations performed to date by PVP95; Ostriker et al. 2001; Padoan et al. 2001; Heitsch et al. 2001) the total mass is fixed. Then, starting with roughly uniform magnetic fields and densities, an initially subcritical box will always be subcritical (and the clouds it forms will be subcritical) in absence of diffusion or reconnection. As emphasized by Heitsch et al. (2001), protostellar collapse is inhibited by magnetic fields if they initially provide magnetohydrostatic support; otherwise, they will slow, but will not stop, collapse.

For a given average magnetic field strength and gas density, the size of the computational region then determines whether the region is subcritical or supercritical. The key parameter is the “accumulation length” (e.g., Mestel 1985), the distance along a magnetic flux tube needed to achieve the critical column density. The accumulation length  $l$  for forming a magnetically critical cloud is roughly

$$l_c \sim 430 \left( \frac{B}{5 \mu\text{G}} \right) \left( \frac{n_{\text{H}}}{1 \text{ cm}^{-3}} \right) \text{pc}, \quad (21)$$

where the fiducial values are typical for the Galactic interstellar magnetic field and hydrogen density in the vicinity of the Sun (Heiles 1995; Mathis 2000; Beck 2001). Thus, for typical ISM values of gas density and magnetic field strength, computational regions larger than about 400 pc will be supercritical as a whole in the absence of diffusion or reconnection.

It seems at least intuitively plausible that the computational “box” for cloud formation should be at least as large as some relevant dimension perpendicular to the Galactic plane, if not larger. A region of at least  $\sim 270$  pc would be required to match one scale height above and below the plane in the atomic hydrogen distribution (Mathis 2000; Dickey & Lockman 1990). A scale of this length is also strongly suggested by the Orion molecular complex, which extends about 140 pc below the Galactic plane. Another important constraint is the overall pressure scale length. Boulares & Cox (1990) have argued that the magnetic pressure in the local ISM at the solar radius drops by only a factor of 2 at distances of  $\pm 400$  pc above and below the plane. Thus, a computational volume with a lateral dimension of one vertical pressure scale height would be approximately magnetically critical at the typical densities and field strengths in the solar neighborhood.

These considerations suggest that the accumulation lengths for molecular clouds are simply large enough that clouds are supercritical when formed. A large accumulation length is also consistent with the results of numerical simulations (PVP95; BHV99; § 4), in which clouds are formed from flows extending over several hundred parsecs. It may not be a coincidence that the formation of a  $10^6 M_{\odot}$  giant

molecular cloud out of diffuse material at  $1 \text{ cm}^{-3}$  requires the accumulation of material from a volume of  $\sim 400$  pc in size (Williams, Blitz, & McKee 2000).

The possibility that clouds can have large enough accumulation lengths to be magnetically supercritical does not mean that they will be supercritical. However, we argue that subcritical clouds generally are not molecular. The internal magnetic pressure (random plus ordered components) must be less than or at most comparable to the external turbulent pressure in the ISM; otherwise, the cloud would expand. Assuming again a sheetlike geometry, the tangential external pressure (along the sheet) needed to confine a magnetic field  $B$  oriented roughly perpendicular to the sheet is

$$P_t \gtrsim \frac{B^2}{8\pi}. \quad (22)$$

Now  $P_t$  will be at most equal to, and more likely less than, the pressure component  $P_e$  normal to the sheet (otherwise, the sheet would become compressed in the opposite direction). However, column densities satisfying equation (8) imply  $G\Sigma^2/2 \gtrsim P_e$ . Thus, when equation (8) is satisfied, we have

$$\frac{G\Sigma^2}{2} \gtrsim P_e \gtrsim P_t \gtrsim \frac{B^2}{8\pi}, \quad (23)$$

which satisfies equation (19). Thus, the cloud tends to be supercritical at column densities high enough for molecular gas formation.

The reason why previous considerations of (strongly) magnetically subcritical clouds do not come to this conclusion is that they do not apply a criterion such as equation (22), and so the magnetic field can be of arbitrary strength. Because the internal magnetic pressure of a subcritical cloud exceeds the force of gravity, such a cloud must expand unless it is confined by external pressure forces (Fiedler & Mouschovias 1993), and it is generally unlikely that external pressure forces can hold a strongly subcritical cloud together (Nakano 1998; Hartmann 1998), particularly if these pressures are turbulent and therefore highly anisotropic and time dependent (BVS99).

It should be emphasized that the above discussion deals mainly with the large scale. In principle it is always possible to find a small enough scale within a supercritical cloud that is subcritical. However, given the importance of boundary conditions as described in the preceding paragraph, we think that the large scale is controlling. If supercritical collapse can proceed on the scale of the cloud, subsequent fragmentation in principle can occur to produce smaller supercritical cores.

### 3.6. Simulation of Cloud Formation

To support the picture of cloud formation outlined above, with particular emphasis on the issue of magnetic field support, we consider the behavior of the Galactic ISM from PVP95 to help support these assumptions. To this end, we display results from a run called r28cfa, which has the same parameters as the fiducial run 28 in PVP95, but performed on a workstation at CfA.<sup>7</sup>

<sup>7</sup> In BHV99 (also Fig. 5) we showed a simulation, called run 28.800, with similar parameters but with higher spatial resolution ( $800^2$  pixels), in which star formation was turned off after 65 Myr.

The simulations consider a two-dimensional section of the ISM in the Galactic plane at the solar circle, which has dimensions of  $1000 \times 1000$  pc, large enough to encompass a critical accumulation length (§ 3.4). The model includes self-gravity, magnetic fields, Coriolis force, Galactic shear, diffuse heating, cooling, and stellar energy input, as well as a scheme for star formation. Details of the model are given in PVP95. We note that (see Table 1 in PVP95 for the standard parameters) the initial conditions are random in all variables with phases uncorrelated. In particular, the magnetic field, which is entirely in the plane of the simulation, has a uniform initial component of  $1.6 \mu\text{G}$  and a random component of  $5 \mu\text{G}$ , corresponding to an initial rms magnetic pressure of  $P_B/k \sim 7 \times 10^3 \text{ cm}^{-3} \text{ K}$ .

Small random perturbations in velocity and density are introduced initially, and then the system is left to evolve. Once the gas reaches densities  $\geq 30 \text{ cm}^{-3}$ , and if the local velocity field is convergent ( $\nabla \cdot \mathbf{u} < 0$ ), star formation is assumed to occur and an energy source corresponding to the energy of massive O stars is turned on for a lapse of time of 6 Myr, the lifetime typical for massive O stars (see Vázquez-Semadeni et al. 1995).

This scheme for star formation has the following “collateral” effects. First of all, it prevents densities from getting much larger than the threshold density for star formation. On the other hand, while the energy input is point-like (i.e., at small scales), its long-term effect (after several megayears) is to drive turbulence at all scales. This is because the “H II regions” of hot gas formed by the newborn stars expand, interact with each other, and form structures at all scales.

Much, if not most, of the stellar energy input into the ISM arises from SNe (Spitzer 1978; Wada & Norman 2001). The simulation presented here does not include such energy input (although there exists a variation of this code that includes SNe; see Gazol-Patiño & Passot 1999). In reality, much of the driving flows are initially in hot, ionized bubbles, rather than the relatively low temperature diffuse atomic flows considered here (e.g., McCray & Kafatos 1987). However, this should not change our general conclusions, since the hot gas must eventually cool and become atomic before it can make a transition to the molecular phase.

The simulation starts at constant density ( $1 \text{ cm}^{-3}$ ) with fluctuations of about 20%. Because the perturbations are uncorrelated, strong shocks appear and form the first low-density clouds. In Figure 6, we show four snapshots of run 28 at  $t = 0, 9, 64,$  and  $117$  Myr. The gray scale indicates regions of increased density; “clouds,” defined as regions where the density exceeds  $15 \text{ cm}^{-3}$ , are outlined by black contours. The magnetic field directions are indicated by the arrows.

The first point to notice in Figure 6 is that the first dense structures formed (*top right panel*) are separated by about 100 pc, and so this corresponds to their accumulation lengths. Evolution from densities of  $1 \text{ cm}^{-3}$  up to densities of  $30 \text{ cm}^{-3}$  takes about 10 Myr; after that, relatively dense clouds are present most of the time. To form the larger and denser clouds in the bottom left and right panels, accumulation has proceeded over larger distance scales. Figure 6 shows that after star formation has proceeded for several tens of megayears, most lines of sight pass through few regions of higher than average density. The dominant flow is in the  $x$ -direction (direction of Galactic rotation); along

any cut at constant  $y$ , there are no clouds, or only one. Even considering regions with lower densities than our “clouds,” there are a relatively small number of structures intercepting a given line at constant  $y$ . This indicates that the scale of accumulation along the  $x$ -direction is a large fraction of the 1 kpc box length, and therefore it is not surprising that the clouds are supercritical.

The simulation shows that star formation is spatially and temporally correlated; once star formation ensues in a given region, some of the dispersed material recondenses nearby (several tens of parsecs distant) a few to tens of megayears later (see also Elmegreen & Efremov 1996). Although the simulation does not address the question directly, we suggest that the disappearance of old clouds and the formation of new clouds result from a combination of actually moving gas from one place to another as well as dissociation and reformation of the molecular material (see § 3.7). This behavior will be analyzed more carefully in a subsequent paper (J. Ballesteros-Paredes et al. 2001, in preparation). Here we merely note that the simulations demonstrate the important distinction between the star-forming history of a region tens to hundreds of parsecs in size and the evolution of an individual parcel of gas. Over a sufficiently large volume, star formation can proceed for tens of megayears even though the individual molecular cloud regions form, produce stars, and disperse more rapidly (e.g., Elmegreen 1979).

The simulations support the point made in § 3.4 that the deceleration of large-scale flows can result in a line-of-sight “turbulent velocity broadening” that does not correspond to internal pressure support, but rather to the compression of the cloud. Such features may be seen in all the clouds in the simulation, as can be seen also in BVS99 (see also the expanded view of a cloud in Fig. 5).

Figure 7 shows the evolution of energies within the entire computational region. The gravitational energy (*solid line*) has the opposite sign to facilitate comparison with the other energies. The magnetic (and internal) energies remain nearly constant for the first 50 Myr of the simulation, decaying slightly thereafter. The overall kinetic energy decreases slightly at first as a result of dissipation and then eventually steadies or even rises as a result of stellar energy input. The main evolution is in the gravitational potential energy in the volume, which rises rapidly until it becomes roughly comparable to the other energy terms.

Figure 8 compares the evolution of the energies of the “clouds,” defined as connected grid cells with densities greater than  $15 \text{ cm}^{-3}$ . Each line in Figure 8 represents the sum over all clouds of various energy components (gravitational, thermal, kinetic, or magnetic). (The kinetic energy for each cloud is calculated in the frame of reference of the cloud itself, i.e., bulk motion is not included.) Figure 8 shows considerable evolution with time of all energy components. The magnetic energy tracks the kinetic and internal energies most closely, as predicted by the pressure argument (eq. [22]); this is made explicit in Figure 9, which converts the values in Figure 8 to cgs pressures by dividing the total energies of the clouds by their total area (since the simulations are two-dimensional). Comparison between Figures 8 and 9 shows that much of the energy evolution in Figure 8 is due to increasing cloud volume (area) rather than changing energies per unit volume (area). The gravitational energies/pressures rise as time progresses, and they exceed the corresponding magnetic values as would be

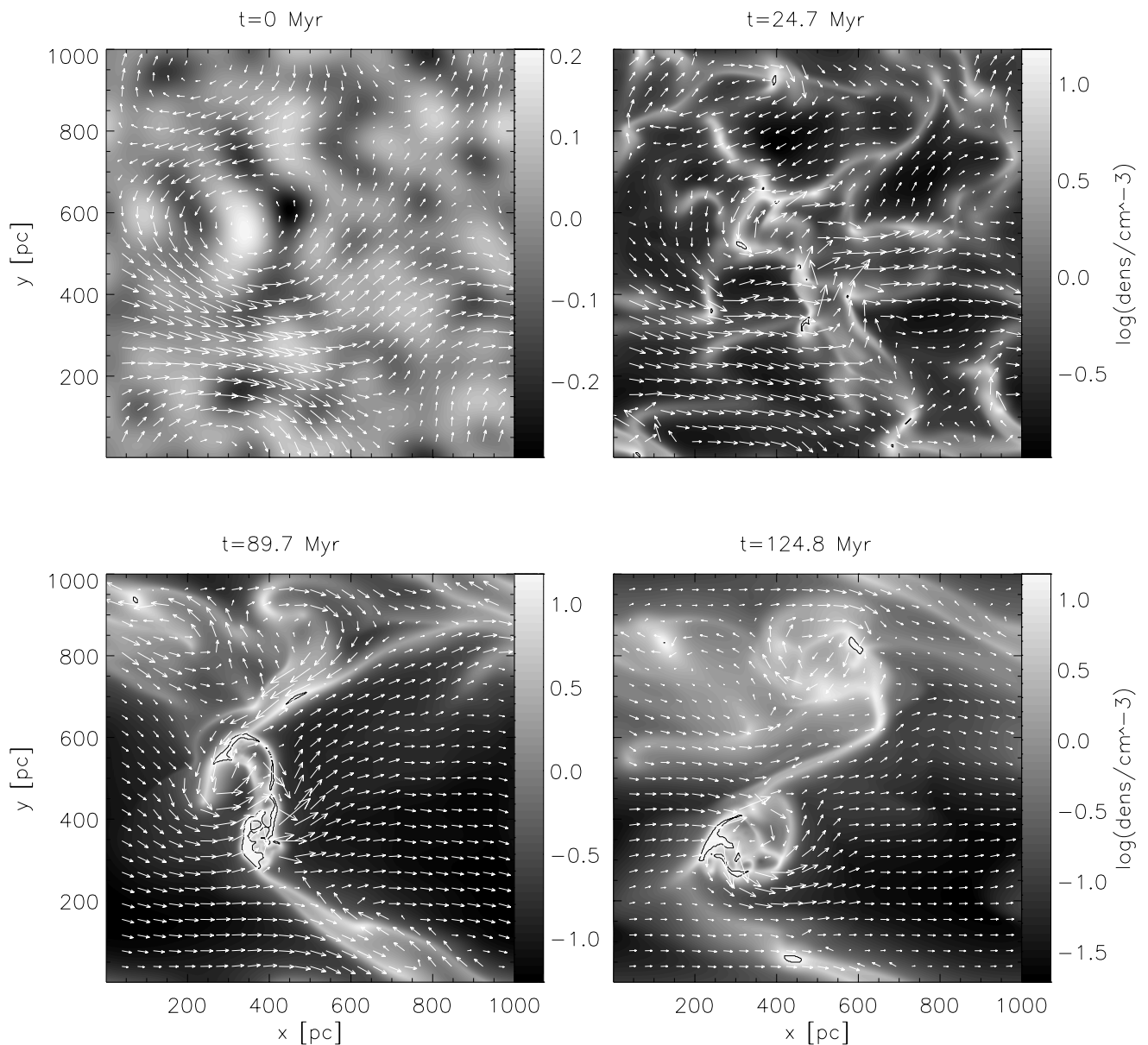


FIG. 6.—Four snapshots of run cfa28 (see text) at  $t = 0$  (top left), 24.7 (top right), 89.7 (bottom left), and 124.8 Myr (bottom right). Vectors indicate magnetic field directions and strengths. The gray scale denotes the density in logarithmic units, as indicated in the gray-scale bars. “Clouds,” defined as regions where the density exceeds  $15 \text{ cm}^{-3}$ , are denoted by the black isocontours. After about 10 Myr, “star formation” occurs in the model (when local densities increase to the threshold level; see text), adding energy to the simulation. Clouds are built up by flows over scales of several hundreds of parsecs, concentrating most of the mass into a small fraction of the computational region.

required by the argument leading to equation (23) for self-gravitating clouds.

Figure 10 compares the magnetic ( $E_m$ ) and (negative) gravitational ( $E_g$ ) energies of individual clouds at three selected times (the same last three time steps in Fig. 6). Again, the magnetic and gravitational energies are correlated, with the larger clouds being dominated by gravitational energy and smaller clouds more likely to be magnetically dominated. This corresponds to the larger clouds being supercritical, as expected from § 3.5.

In assessing criticality, we compare energies rather than use the mass-to-flux relation (eq. [19]). However, virial theorem arguments for flattened clouds give essentially the same result as the force perturbation analysis for the sheet (Nakano & Nakamura 1978; Strittmatter 1966). Note that

the mass-to-flux criterion relates  $B$  to cloud mass  $M$ , whereas the energies in Figure 6 involve squares of these quantities; thus, the results shown in Figure 10 correspond to clouds that are within factors of a few of critical, as indicated by observations (e.g., Crutcher 1999).

It is possible that hyperviscosity used in the scheme helps remove some magnetic flux and thus tends to make clouds in the simulation more supercritical than they should be. However, the large accumulation lengths of the clouds in the simulation compared to the small scales on which the hyperviscosity matters (Vazquez-Semadeni et al. 1995) suggest that the latter is not the essential factor in making supercritical clouds. This is corroborated by the fact that the total magnetic energy over the entire simulation has a very small decrease over the 130 Myr. In summary, the

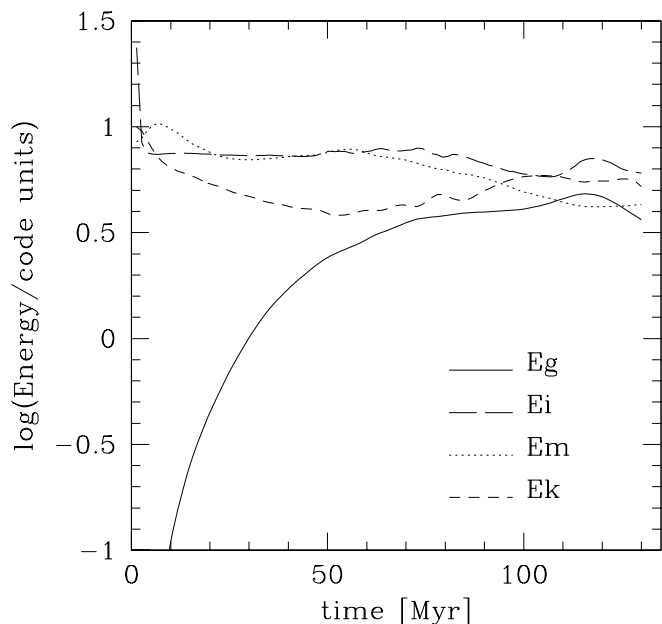


FIG. 7.—Evolution of (negative) gravitational ( $E_g$ ; solid line), thermal ( $E_i$ ; long-dashed line), magnetic ( $E_m$ ; dotted line), and kinetic ( $E_k$ ; short-dashed line) energies for the whole computational domain. Note that the internal energies are larger than the gravitational energy, indicating that the whole computational domain is supported against collapse.

results of the numerical simulations tend to support the idea that molecular clouds will be supercritical as a result of large accumulation lengths.

### 3.7. Dispersal

It is evident that rapid cloud dispersal after the onset of star formation is a crucial part of the explanation of why

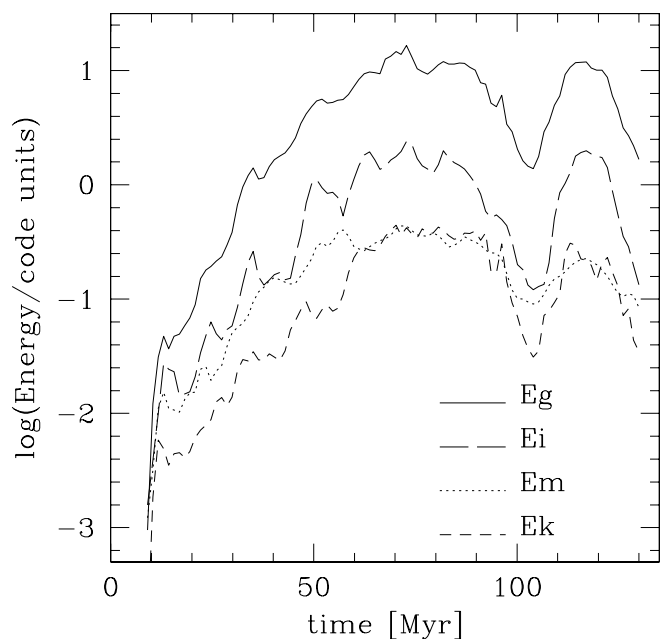


FIG. 8.—Similar to Fig. 7, but for clouds (connected set of pixels with densities above  $15 \text{ cm}^{-3}$ ). Note that in this case the larger energy is the gravitational, indicating that the clouds are not supported against gravity and can collapse rapidly. The kinetic energy is calculated in the frame of reference of the cloud.

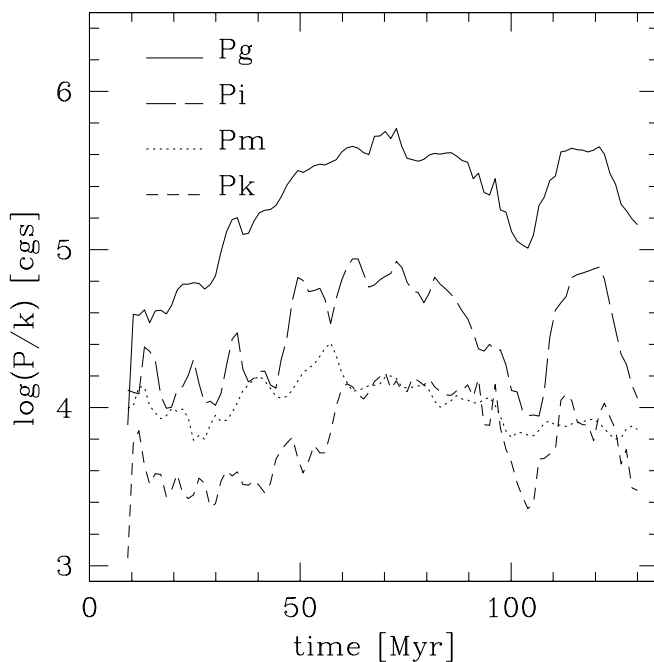


FIG. 9.—Evolution of the pressures for the clouds in the simulation. Each pressure is calculated as the energy divided by its volume (in the present case, by its area, since the simulations are two-dimensional), such that even the gravitational energy has its counterpart in pressure. In this case, the gravitational pressure has to be considered as a compressible pressure, since the effect of gravity is the opposite to the magnetic or thermal pressure. The kinetic energy component in general includes the compressible (contraction, expansion) and the incompressible (rotational) components. Note that the values of the typical pressures (magnetic, kinetic, and thermal) are  $P/k \sim 10^3\text{--}10^4 \text{ cm}^{-3} \text{ K}$ . Comparison with Fig. 8 indicates that much of the cloud energy evolution is mostly due to changing cloud volumes (areas).

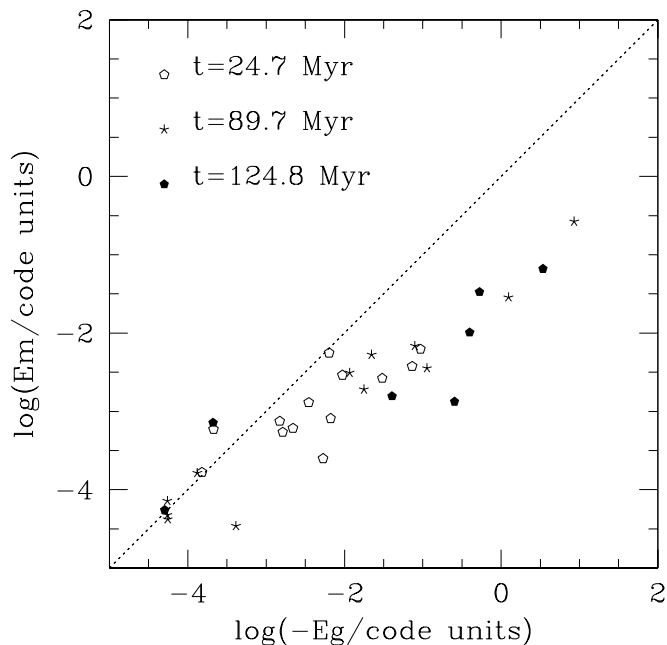


FIG. 10.—Magnetic vs. gravitational energy for clouds in the last three time steps in Fig. 6 ( $t = 24.7, 89.7,$  and  $124.8 \text{ Myr}$ ). Note that while the energies are comparable and correlated, the gravitational energy is somewhat larger for more massive clouds, implying that they are magnetically supercritical (see text).

star-forming populations in molecular clouds are young. If massive (O) stars are present, or if a nearby SN explosion has occurred, removing the remaining gas on a few megayears is no problem (e.g., Cep OB2, Patel et al. 1998; also the  $\lambda$  Ori cluster, Dolan & Mathieu 1999). Dispersal of molecular clouds by low-mass stars is another matter. The power of a group of low-mass stars to eject material is uncertain but is probably much smaller than that of a single O star. Moreover, the efficiency of star formation appears to be much higher in high-density regions producing high-mass stars, and thus the low-mass stars need to disperse much more gas relative to the total mass in stars.

The outflows of young low-mass, PMS stars can eject material, as long as the outflow is not simply confined to a narrow, highly collimated jet, but exerts significant ram pressure over at least a moderate solid angle (e.g., Matzner & McKee 1999, 2000). Matzner & McKee (2000) suggest that outflows from low-mass stars might result in star formation efficiencies of  $\sim 30\%$ ; in other words, these stars might be able to prevent twice their mass in external gas from forming other stars. However, this level of mass ejection would not explain the low efficiencies of a few percent in many star-forming regions (Cohen & Kuhl 1979).

In general, the mass-loss rates of TTSs and FU Ori objects are consistent with about 10% of the accreted mass being ejected (Calvet 1991). Let us assume that this ratio of mass ejected to accreted characterizes the entire star formation process. The outflows almost certainly dissipate most of their energy in radiative shocks, so that momentum conservation is the relevant consideration for dispersal of molecular gas. If the typical wind velocity is assumed to be  $\sim 200 \text{ km s}^{-1}$ , then in principle an amount of mass  $\sim 100$  times as large as that ejected can be swept up in shells to velocities  $\sim 2 \text{ km s}^{-1}$ , comparable to the escape velocities from typical molecular cloud complexes. This would imply a possible ejection of 10 times as much mass as formed into stars, or a star formation efficiency of  $\sim 10\%$ . This is slightly smaller than the Matzner & McKee (2000) estimate, but still higher than the  $\sim 1\%$ – $2\%$  found in Taurus and other regions.

In addition, unless the flows eject the molecular gas at  $\approx 10 \text{ km s}^{-1}$ , gas cannot be dispersed spatially very far on timescales of a few megayears. Essentially, this is the inverse of the formation problem. If ejection did occur at high velocities, the amount of cloud mass that could be dispersed would be strongly reduced because most of the kinetic energy of the flow would be dissipated in the (radiative) shock as it sweeps up molecular material.

The reduction of shielding almost certainly plays an important role in the “disappearance” of molecular gas near young, low-mass stars. Molecular clouds are not spherical; they must be clumpy (e.g., Blitz & Shu 1980; Kwan & Sanders 1986; Hollenbach & Tielens 1999) and often appear filamentary (e.g., Fig. 2) or even fractal (see Elmegreen 1997 and references therein). If the stellar energy input can expand the surface area of the dense gas sufficiently, the reduction in shielding can dissociate the molecular gas. Actually, Elmegreen (1997) estimated that radiation from an ionizing O star can travel twice as far as otherwise would be expected if the clouds are fractal, with a small filling factor. In the inverse process to cloud formation, dispersal can result in turning the gas into atomic form so that it is difficult to observe. For regions like Taurus, where the typical extinctions are  $A_V \sim 1$ – $2$  (e.g., Arce & Goodman

1999), an expansion of surface area of only a factor of 2–3, with a consequent reduction of column density by the same factor, could suffice to turn much of the molecular gas atomic (eq. [2]). In this case it is necessary to expand the gas by only a few parsecs in a few megayears to make the molecular cloud “disappear.” This effect is also important in high-mass regions, as the photodissociating and photoionizing fluxes of massive young stars will generally eliminate molecular gas long before the actual material is dispersed to large distances.

Thus, rapid dispersal of low-mass star-forming molecular clouds by stellar winds is possible, though uncertain in its actual efficiency. It may be that low surface density molecular clouds are so lightly bound gravitationally that the injection of even modest amounts of stellar energy suffices to disrupt them. Perhaps external ram pressure forces also assist in injecting additional turbulent energy that makes star formation efficiencies low to begin with. It is interesting that in Taurus, the molecular gas seems to extend systematically west of the TTSs (Fig. 2). Is the gas being blown systematically away from the stars in this direction? In any event, it is clear from several of the small groups in Taurus (for instance, the groups at  $b \sim -10$ ,  $l \sim 178$  and the L1551 group at  $b \sim -20$ ,  $l \sim 179$ ) that the molecular gas is being swept away rapidly as a result of some mechanism. Perhaps large-scale turbulent flows, in addition to forming clouds, may help disrupt the least tightly bound complexes. In any event, the problem of rapid dispersal of molecular gas in low-mass, low-density clouds remains one of the biggest challenges to the picture presented here.

### 3.8. Summary Outline of Rapid Cloud and Star Formation

To explain the small age spreads (less than lateral crossing times) of spatially extended star-forming regions and stellar associations, large-scale (hundreds of parsecs) flows must be involved in forming molecular clouds (e.g., McCray & Kafatos 1987; PVP95; BHV99). These flows may take tens of megayears to accumulate enough mass to form stars, but the resulting clouds become molecular only when column densities and volume densities reach threshold values. At these levels of column density and volume density, gravitational forces are important relative to external and internal pressure support. As shown in recent numerical simulations, rapid dissipation of turbulence is likely to allow gravitational collapse to occur, at least in restricted regions, with timescales of a few megayears or less at threshold column densities. The large-scale nature of the flows leads to large accumulation lengths, increasing mass-to-flux ratios; this feature, plus pressure balance constraints, implies that clouds are generally both self-gravitating and magnetically supercritical when they become molecular, and thus ambipolar diffusion reduction of magnetic flux is not an essential feature of star formation.

## 4. DISCUSSION

### 4.1. Large-Scale Structures

The probable importance of high-velocity flows driving cloud formation in the ISM is supported by the existence of molecular gas structures that lie considerable distances out of the Galactic plane. The recent large-scale CO map of the galaxy by Dame, Hartmann, & Thaddeus (2001) gives the impression that the Orion A and B clouds are part of a bubble extending below the Galactic plane. Whether or not

this is the case, some mechanism is required to move the gas as much as 140 pc out of the Galactic plane; driving by stellar/SN energy input can naturally produce such structures (see, e.g., Shapiro & Field 1976, or more recent numerical simulations by de Avillez 2000; de Avillez & Mac Low 2001). It has been suggested that the Orion complex is the result of a high-velocity cloud crashing into the Galactic plane (e.g., Franco et al. 1988), but flows from stars/SNe are at least an equally probable, if not more plausible, explanation. In this connection one wonders if the stars in the Gould Belt (Pöppel 1997) were not produced in clouds created by complex interacting flow patterns moving material around and out of the Galactic plane, accidentally producing a structure that appears coherent and tilted with respect to the plane.

In this connection we note that Olano & Pöppel (1987) suggested that the Taurus clouds might have formed as part of the general expansion of the gas responsible for the Gould Belt. However, the age of the stellar population in Taurus (§ 2.1) is much smaller than the age ( $18 \pm 3$  Myr) suggested by Olano & Pöppel (1987). More generally, our simulations of the ISM (and others) demonstrate the importance of large-scale flows (see Fig. 5), so that the Olano & Pöppel (1987) model of a shell snowplowing into a static medium is highly unrealistic. Because of the overlapping of long-range flows, efforts to attribute cloud origins to single events or structures will generally fail.

The picture presented here, although envisioning cloud formation over hundreds of parsecs, is basically a local one compared with spiral arm structure. Spiral arms clearly play a role in star formation by accumulating gas, and in principle a spiral wave shock is just as good as an SN or stellar wind-driven shock for compressing gas. In our picture, the energy put into the ISM by massive stars rapidly produces more complex structure within the spiral arm, as, for example, in the picture outlined by Elmegreen (1979), in which individual molecular cloud regions form, produce stars, and disperse more rapidly within the general arm region.

An important part of our explanation of the rapidity with which stars form after molecular gas formation is the notion that the flows are initially atomic and only become molecular when sufficient column density has been accumulated. This picture of atomic to molecular gas conversion is most appropriate near the solar circle, where most of the gas is atomic; it may not be relevant for inner regions in our Galaxy, where the molecular component dominates, or more generally in other galaxies with different ratios of atomic and molecular gas (Pringle, Allen, & Lubow 2001). However, rapid star formation is likely to be appropriate in any case (Elmegreen 2000; Pringle et al. 2001), although difficult to prove in the absence of sufficiently precise stellar population ages.

#### 4.2. *Supercritical Star Formation*

The picture we have outlined above is at variance with the standard model of low-mass star formation. The standard picture assumes that stars form in dark clouds because it is only in such regions that the ionization decreases to a level where ambipolar diffusion can proceed (Shu et al. 1987; Bertoldi & McKee 1996). Instead, we suggest that dark molecular clouds are the sites of star formation because they represent a stage of cloud evolution closer to stellar densities than represented by the atomic phase,

partly as a result of turbulent energy dissipation. Furthermore, we argue that molecular clouds form in a magnetically supercritical state (§ 3.4) and therefore ionization effects on ambipolar diffusion rates are generally not important.

Sometimes it is argued that, although molecular cloud complexes are supercritical as a whole, star formation proceeds from subcritical units within such cloud complexes (e.g., McKee et al. 1993). It seems more plausible to assume that gravitational collapse occurs first in supercritical regions; subcritical regions may be disrupted by stellar energy input before enough ambipolar diffusion can occur to permit gravitational collapse (Hartmann 1998).

#### 4.3. *Efficiency and Galactic Star Formation Rates*

It follows from the above that the low rate of Galactic star formation is not the result of slowing by ambipolar diffusion of magnetic fields through dense gas; instead, it is the result of a low efficiency in converting gas into stars (Hartmann 1998; Elmegreen 2000). The rapid dispersal of clouds may be the main factor determining the efficiency. It is much easier to see how turbulent flows powered by stellar energy input would form, shape, and disrupt clouds than trying to maintain a quasi-equilibrium configuration that would allow clouds to survive for long periods; and this is why, as shown by observations (§ 2), clouds do not have long lifetimes.

The idea that stellar ionization energy and winds are responsible for limiting the efficiency of star formation initially seems to be in conflict with the high star-forming efficiencies of dense regions (Lada & Lada 1991), which form disruptive high-mass stars. However, stellar winds and SNe can have a powerful impact on very large scales, and it can be much easier to eject distant but low-density gas, while very dense natal material can be much more difficult to disperse, even if it is nearby. Cep OB2 (Patel et al. 1998) and other regions show how the large-scale effects of stellar energy input can clear out atomic and molecular gas over many tens of parsecs on timescales of 10 Myr that otherwise might eventually collapse gravitationally if left undisturbed.

#### 4.4. *Protostellar Collapse*

Another implication of our picture is that slow models of star formation, where cores in hydrostatic equilibrium evolve slowly over many dynamical timescales before collapsing, generally are not appropriate. The flow-driven model predicts that, since the newly formed molecular cloud is almost immediately susceptible to gravitational collapse, as well as being compressed by external flows, it would be natural to observe systematic motions of contraction on large scales. The large-scale infall motions discussed by Williams & Myers (2000) could be a natural consequence of our model.

Although protostellar cloud cores are often modeled as hydrostatic structures, it is difficult to imagine conceptually how flow-driven cloud formation would produce such static, slowly evolving structures. In fact, as BVS99 show, hydrostatic equilibrium cannot be obtained in turbulent flows until protostellar densities are reached. Stars can be formed by dynamic processes and still rapidly achieve hydrostatic equilibrium because their cooling times are many orders of magnitude longer than their characteristic free-fall times; thus, the energy dissipated by shocks can be internalized and diffused within a static interior. Molecular

clouds and cores do not share this property. Shocks in the supersonic flows can and do dissipate turbulence to relatively low levels, but true hydrostatic equilibrium is highly unlikely. Indeed, core statistics do not seem to suggest that they are very long lived entities (Lee & Myers 1999).

Protostellar cores generally are not spherical and may even have a tendency to be prolate<sup>8</sup> (Jijina et al. 1999), which is much easier to explain if cores are not in hydrostatic equilibrium (Fleck 1992). Jones, Basu, & Dubinski (2001) recently have argued that cores are generally triaxial, closer to prolate, and thus closer to a sustainable hydrostatic equilibrium than previously thought. However, a dynamic picture would also naturally lead to an approximate “triaxiality” (i.e., all dimensions differing) without requiring any special conditions.

Therefore, our flow-driven, rapid star formation picture is consistent with the view that cloud cores are formed, at least in part, by the collision of large-scale supersonic flows within molecular clouds (Elmegreen 1993a; PVP95; BVS99; Padoan et al. 2001), giving rise to clustered star formation (Klessen et al. 2000; see also Elmegreen et al. 2000).

## 5. CONCLUSIONS

The evidence of stellar populations shows that molecular clouds in the solar neighborhood generally form rapidly, produce stars rapidly, and disperse quickly, all within a timescale of only a few megayears. In some cases, the age spread of the young stars is much smaller than the lateral crossing time. We have shown that this surprising behavior can be understood in the context of cloud formation driven by large-scale flows in the ISM caused by global stellar winds and SNe. To understand the observations, it is necessary to account for the conversion from atomic to molecu-

<sup>8</sup> If not fractal, since the sizes of these cores are only few times the beam size used in the observations.

lar gas and back again. The observational requirement for rapid star formation can be satisfied because the column densities necessary for formation of molecular gas are comparable to those required for self-gravity to become important in the solar neighborhood and because collapse times can be as short as 1 Myr under these conditions. Our picture requires that magnetic fields, while having important dynamical effects, do not substantially slow or prevent collapse in at least some portions of molecular clouds; we have presented both general theoretical arguments and numerical simulations in favor of this conclusion.

While we have sketched a plausible explanation of the observations, much more work remains before the picture of rapid star formation can be placed on a firmer theoretical basis. One issue is whether the outflows from low-mass stars can effectively disperse low-density star-forming regions on the required short timescales. The rapid dissipation of small-scale turbulence is required by our picture, and while there is some current justification for this assumption, many details remain uncertain. Finally, the application of flow-driven star formation to higher pressures and densities than considered here, with ultimate application to understanding the formation of high-mass stars and clusters, has yet to be undertaken.

We are grateful to John Black for an extremely detailed and thorough “very rough draft” on the topic of H<sub>2</sub> formation. We also thank Mordecai Mac Low for comments on the manuscript and Ellen Zweibel for useful conversations. Tom Megeath and Tom Dame graciously gave permission to display Taurus <sup>12</sup>CO results, and the latter provided references on gas column densities in the solar neighborhood. We also acknowledge a useful and thorough report from the referee, Bruce Elmegreen. L. H. acknowledges the support from NASA Origins of Solar Systems grant NAG 5-9670. J. B. acknowledges support from NASA Astrophysical Theory Program grant NAG 5-10103 and CONACYT grant 88046-EUA.

## REFERENCES

- Arce, H. G., & Goodman, A. A. 1999, *ApJ*, 517, 264  
 Arquilla, R., & Goldsmith, P. F. 1986, *ApJ*, 303, 356  
 Ballesteros-Paredes, J. 1999, Ph.D. thesis, Universidad Nacional Autónoma de México  
 ———. 2000, in 33d ESALAB Symp., *Star Formation from the Small to the Large Scale*, ed. F. Favata, A. Kaas, & A. Wilson (ESA SP-445; Noordwijk: ESA), 323  
 Ballesteros-Paredes, J., Hartmann, L., & Vazquez-Semadeni, E. 1999a, *ApJ*, 527, 285 (BHV99)  
 Ballesteros-Paredes, J., & Mac Low, M. 2001, *ApJ*, submitted  
 Ballesteros-Paredes, J., & Vazquez-Semadeni, E. 1995, *Revista Mexicana de Astronomía y Astrofísica Conf. Ser.* 3, 105  
 ———. 1997, in *AIP Conf. Ser.* 393, *Star Formation Near and Far*, ed. S. S. Holt & L. G. Mundy (New York: AIP), 81  
 Ballesteros-Paredes, J., Vázquez-Semadeni, E., & Scalo, J. 1999b, *ApJ*, 515, 286 (BVS99)  
 Beck, R. 2001, *Space Sci. Rev.*, in press  
 Bergin, E. A., Langer, W. D., & Goldsmith, P. F. 1995, *ApJ*, 441, 222  
 Bertoldi, F., & McKee, C. F. 1996, in *Amazing Light: A Volume Dedicated to C. H. Townes on his 80th Birthday*, ed. R. Y. Chiao (New York: Springer), 41  
 Blaauw, A. 1960, in *Present Problems Concerning the Structure and Evolution of the Galactic System* (Nuffic Intern. Summer Course; The Hague), III.1  
 ———. 1964, *ARA&A*, 2, 213  
 ———. 1991, in *The Physics of Star Formation and Early Stellar Evolution*, ed. C. J. Lada & N. D. Kylafis (Dordrecht: Kluwer), 125  
 Blitz, L., & Shu, F. H. 1980, *ApJ*, 238, 148  
 Boulares, A., & Cox, D. P. 1990, *ApJ*, 365, 544  
 Bourke, T. L., Myers, P. C., Robinson, G., & Hyland, A. R. 2001, *ApJ*, 554, 916  
 Briceño, C., Calvet, N., Kenyon, S., & Hartmann, L. 1999, *AJ*, 118, 1354  
 Briceño, C., Hartmann, L. W., Stauffer, J. R., Gagne, M., Stern, R. A., & Caillault, J. 1997, *AJ*, 113, 740  
 Burton, M. G., Hollenbach, D. J., & Tielens, A. G. G. M. 1990, *ApJ*, 365, 620  
 Calvet, N. 1991, in *IAU Colloq.* 129, *Structure and Emission Properties of Accretion Disks*, ed. C. Bertout, S. Collin-Souffrin, & J. P. Lasota (San Francisco: ASP), 343  
 Chandrasekhar, S., & Fermi, E. 1953, *ApJ*, 118, 116  
 Ciolek, G. E., & Basu, S. 2001, *ApJ*, 547, 272  
 Cohen, M., & Kuhl, L. V. 1979, *ApJS*, 41, 743  
 Crutcher, R. M. 1999, *ApJ*, 520, 706  
 Dame, T. M. 1993, in *AIP Conf. Proc.* 278, *Back to the Galaxy*, ed. S. S. Holt & F. Verter (New York: AIP), 267  
 Dame, T. M., Hartmann, D., & Thaddeus, P. 2001, *ApJ*, 547, 792  
 D’Antona, F., & Mazzitelli, I. 1994, *ApJS*, 90, 467  
 de Avillez, M. A. 2000, *MNRAS*, 315, 479  
 de Avillez, M. A., & Mac Low, M. 2001, *ApJ*, 551, L57  
 de Bruijne, J. H. J. 1999, *MNRAS*, 310, 585  
 de Geus, E. J., de Zeeuw, P. T., & Lub, J. 1989, *A&A*, 216, 44  
 de Zeeuw, P. T., Hoogerwerf, R., de Bruijne, J. H. J., Brown, A. G. A., & Blaauw, A. 1999, *AJ*, 117, 354  
 Dickey, J. M., & Lockman, F. J. 1990, *ARA&A*, 28, 215  
 Dolan, C. J., & Mathieu, R. D. 1999, *AJ*, 118, 2409  
 Eaton, N., Rolph, C. D., Scarrott, S. M., & Wolstencroft, R. D. 1990, *MNRAS*, 244, 527  
 Elmegreen, B. G. 1979, *ApJ*, 231, 372  
 ———. 1991, in *NATO ASIC 342, The Physics of Star Formation and Early Stellar Evolution*, ed. C. J. Lada & N. J. Kylafis (Dordrecht: Kluwer), 35  
 ———. 1993a, *ApJ*, 419, L29  
 ———. 1993b, in *Protostars and Planets III*, ed. E. H. Levy & J. I. Lunine (Tucson: Univ. Arizona Press), 97

- Elmegreen, B. G. 1997, *ApJ*, 477, 196  
 ———. 2000, *ApJ*, 530, 277
- Elmegreen, B. G., & Efremov, Y. N. 1996, *ApJ*, 466, 802
- Elmegreen, B. G., Efremov, Y., Pudritz, R. E., & Zinnecker, H. 2000, in *Protostars and Planets IV*, ed. V. Mannings, A. P. Boss, & S. S. Russell (Tucson: Univ. Arizona Press), 179
- Elmegreen, B. G., & Elmegreen, D. M. 1978, *ApJ*, 220, 1051
- Elmegreen, B. G., & Lada, C. J. 1977, *ApJ*, 214, 725
- Feigelson, E. D. 1996, *ApJ*, 468, 306
- Fiedler, R. A., & Mouschovias, T. C. 1993, *ApJ*, 415, 680
- Fleck, R. C. 1992, *ApJ*, 401, 146
- Franco, J., & Cox, D. P. 1986, *PASP*, 98, 1076
- Franco, J., Tenorio-Tagle, G., Bodenheimer, P., Rozyczka, M., & Mirabel, I. F. 1988, *ApJ*, 333, 826
- Gazol-Patiño, A., & Passot, T. 1999, *ApJ*, 518, 748
- Goldreich, P., & Lynden-Bell, D. 1965a, *MNRAS*, 130, 97  
 ———. 1965b, *MNRAS*, 130, 125
- Gomez, M., Jones, B. F., Hartmann, L., Kenyon, S. J., Stauffer, J. R., Hewett, R., & Reid, I. N. 1992, *AJ*, 104, 762
- Hartmann, L. 1998, in *Accretion Processes in Star Formation* (Cambridge: Cambridge Univ. Press), 33  
 ———. 2000, in *33d ESALAB Symp., Star Formation from the Small to the Large Scale*, ed. F. Favata, A. Kaas, & A. Wilson (ESA SP-445; Noordwijk: ESA), 107  
 ———. 2001, *AJ*, 121, 1030
- Hartmann, L., Jones, B. F., Stauffer, J. R., & Kenyon, S. J. 1991, *AJ*, 101, 1050
- Heiles, C. 1995, in *ASP Conf. Ser. 80, The Physics of the Interstellar Medium and Intergalactic Medium*, ed. A. Ferrara, C. F. McKee, C. Heiles, & P. R. Shapiro (San Francisco: ASP), 507
- Heitsch, F., Mac Low, M., & Klessen, R. S. 2001, *ApJ*, 547, 280
- Hennebelle, P., & Pérault, M. 2000, *A&A*, 359, 1124
- Herbig, G. H. 1978, in *Problems of Physics and Evolution of the Universe*, ed. L. V. Mirzoyan (Yerevan: Acad. Sci. Armenian SSR), 171  
 ———. 1998, *ApJ*, 497, 736
- Herbig, G. H., Vrba, F. J., & Rydgren, A. E. 1986, *AJ*, 91, 575
- Hollenbach, D. J., & Tielens, A. G. G. M. 1999, *Rev. Mod. Phys.*, 71, 173
- Hollenbach, D., Werner, M. W., & Salpeter, E. E. 1971, *ApJ*, 163, 165
- Jijina, J., Myers, P. C., & Adams, F. C. 1999, *ApJS*, 125, 161
- Jones, B. F., & Herbig, G. H. 1979, *AJ*, 84, 1872
- Jones, C. E., Basu, S., & Dubinski, J. 2001, *ApJ*, 551, 387
- Jura, M. 1975, *ApJ*, 197, 575
- Kenyon, S. J., & Hartmann, L. W. 1990, *ApJ*, 349, 197  
 ———. 1995, *ApJS*, 101, 117
- Kleiner, S. C., & Dickman, R. L. 1985, *ApJ*, 295, 466
- Klessen, R. S., & Burkert, A. 2001, *ApJ*, 549, 386
- Klessen, R. S., Heitsch, F., & Mac Low, M. 2000, *ApJ*, 535, 887
- Koyama, H., & Inutsuka, S. 2000, *ApJ*, 532, 980
- Kwan, J., & Sanders, D. B. 1986, *ApJ*, 309, 783
- Lada, C. J., & Lada, E. A. 1991, in *ASP Conf. Ser. 13, The Formation and Evolution of Star Clusters*, ed. K. Janes (San Francisco: ASP), 3
- Lagache, G., Abergel, A., Boulanger, F., & Puget, J.-L. 1998, *A&A*, 333, 709
- Larson, R. B. 1981, *MNRAS*, 194, 809
- Ledoux, P. 1951, *Ann. d'Astrophys.*, 14, 438
- Lee, C. W., & Myers, P. C. 1999, *ApJS*, 123, 233
- Leorat, J., Passot, T., & Pouquet, A. 1990, *MNRAS*, 243, 293
- Luhman, K. L. 2001, *ApJ*, 560, 287
- Mac Low, M.-M. 1999, *ApJ*, 524, 169
- Mac Low, M.-M., Klessen, R. S., Burkert, A., & Smith, M. D. 1998, *Phys. Rev. Lett.*, 80, 275
- Mamajek, E. E., Lawson, W. A., & Feigelson, E. D. 1999, *ApJ*, 516, L77  
 ———. 2000, *ApJ*, 544, 356
- Martín, E. L., & Magazzù, A. 1999, *A&A*, 342, 173
- Mathis, J. S. 2000, in *Cox, A. 2000, Allen's Astrophysical Quantities* (4th ed.; New York: Springer), 523
- Matzner, C. D., & McKee, C. F. 1999, *ApJ*, 526, L109  
 ———. 2000, *ApJ*, 545, 364
- McCray, R., & Kafatos, M. 1987, *ApJ*, 317, 190
- McKee, C. F. 1989, *ApJ*, 345, 782
- McKee, C. F., & Hollenbach, D. J. 1980, *ARA&A*, 18, 219
- McKee, C. F., Zweibel, E. G., Goodman, A. A., & Heiles, C. 1993, in *Protostars and Planets III*, ed. E. H. Levy & J. L. Lunine (Tucson: Univ. Arizona Press), 327
- Mestel, L. 1985, in *Protostars and Planets II*, ed. D. C. Black & M. S. Matthews (Tucson: Univ. Arizona Press), 320
- Mouschovias, T. Ch. 1991, in *The Physics of Star Formation and Early Stellar Evolution*, ed. C. J. Lada & N. D. Kylafis (Dordrecht: Kluwer), 61, 449
- Myers, P. C., & Khersonsky, V. K. 1995, *ApJ*, 442, 186
- Nakano, T. 1998, *ApJ*, 494, 587
- Nakano, T., & Nakamura, T. 1978, *PASJ*, 30, 671
- Neuhäuser, R., Sterzik, M. F., Schmitt, J. H. M. M., Wichmann, R., & Krautter, J. 1995, *A&A*, 295, L5
- Norman, C. A. 1995, in *ASP Conf. Ser. 80, The Physics of the Interstellar Medium and Intergalactic Medium*, ed. A. Ferrara, C. F. McKee, C. Heiles, & P. R. Shapiro (San Francisco: ASP), 582
- Nyman, L.-A. 1991, in *ESO Scientific Rep. 11, Low Mass Star Formation in Southern Molecular Clouds*, ed. B. Reipurth (Garching: ESO), 119
- Olano, C. A., & Pöppel, W. G. L. 1987, *A&A*, 179, 202
- Ostriker, E. C., Gammie, C. F., & Stone, J. M. 1999, *ApJ*, 513, 259
- Ostriker, E. C., Stone, J. M., & Gammie, C. F. 2001, *ApJ*, 546, 980
- Padoan, P., Juvella, M., Goodman, A. A., & Nordlund, A. 2001, *ApJ*, 553, 227
- Padoan, P., & Nordlund, Å. 1999, *ApJ*, 526, 279
- Palla, F., & Galli, D. 1997, *ApJ*, 476, L35
- Palla, F., & Stahler, S. W. 2000, *ApJ*, 540, 255
- Passot, T., Vazquez-Semadeni, E., & Pouquet, A. 1995, *ApJ*, 455, 536 (PVP95)
- Patel, N. A., Goldsmith, P. F., Heyer, M. H., Snell, R. L., & Pratap, P. 1998, *ApJ*, 507, 241
- Patel, N. A., Goldsmith, P. F., Snell, R. L., Hezel, T., & Xie, T. 1995, *ApJ*, 447, 721
- Poppel, W. 1997, *Fundam. Cosmic Phys.*, 18, 1
- Preibisch, T., Günther, E., & Zinnecker, H. 2001, *AJ*, 121, 1040
- Preibisch, T., & Zinnecker, H. 1999, *AJ*, 117, 2381
- Pringle, J. E., Allen, R. J., & Lubow, S. H. 2001, *MNRAS*, in press (astro-ph/0106420)
- Sasao, T. 1973, *PASJ*, 25, 1
- Scalo, J., & Chappell, D. 1999, *MNRAS*, 310, 1
- Shapiro, P. R., & Field, G. B. 1976, *ApJ*, 205, 762
- Shu, F. H., Adams, F. C., & Lizano, S. 1987, *ARA&A*, 25, 23
- Siess, L., Dufour, E., & Forestini, M. 2000, *A&A*, 358, 593
- Simon, M., Dutrey, A., & Guilloteau, S. 2000, *ApJ*, 545, 1034
- Simon, R. 1965, *Ann. d'Astrophys.*, 28, 40
- Sodroski, T. J., et al. 1997, *ApJ*, 480, 173
- Spitzer, L. 1978, in *Physical Processes in the Interstellar Medium* (New York: Wiley), 295
- Stone, J. M., Ostriker, E. C., & Gammie, C. F. 1998, *ApJ*, 508, L99
- Strittmatter, P. A. 1966, *MNRAS*, 132, 359
- Tielens, A. G. G. M., & Allamandola, L. J. 1987, in *Interstellar Processes*, ed. D. J. Hollenbach & H. A. Thronson, Jr. (Dordrecht: Reidel), 397
- Tielens, A. G. G. M., & Hollenbach, D. J. 1985, *ApJ*, 291, 722
- Toomre, A. 1981, in *The Structure and Evolution of Normal Galaxies*, ed. S. M. Fall & D. Lynden-Bell (Cambridge: Cambridge Univ. Press), 111
- van Dishoeck, E. F., & Black, J. H. 1988, *ApJ*, 334, 771
- van Dishoeck, E. F., & Blake, G. A. 1998, *ARA&A*, 36, 317
- Vazquez-Semadeni, E., Passot, T., & Pouquet, A. 1995, *Revista Mexicana de Astronomia y Astrofisica Conf. Ser.* 3, 61
- Vishniac, E. T. 1983, *ApJ*, 274, 152
- Wada, K., & Norman, C. A. 2001, *ApJ*, 547, 172
- Walter, F. M., Brown, A., Mathieu, R. D., Myers, P. C., & Vrba, F. J. 1988, *AJ*, 96, 297
- Webb, R. A., Zuckerman, B., Platais, I., Patience, J., White, R. J., Schwartz, M. J., & McCarthy, C. 1999, *ApJ*, 512, L63
- White, R. J., & Ghez, A. M. 2001, *ApJ*, 556, 265
- Wichmann, R., et al. 1996, *A&A*, 312, 439  
 ———. 2000, *A&A*, 359, 181
- Williams, J. P., Blitz, L., & McKee, C. F. 2000, in *Protostars and Planets IV*, ed. V. Mannings, A. P. Boss, & S. S. Russell (Tucson: Univ. Arizona Press), 97
- Williams, J. P., & Myers, P. C. 2000, *ApJ*, 537, 891
- Wolfire, M. G., Hollenbach, D., McKee, C. F., Tielens, A. G. G. M., & Bakes, E. L. O. 1995, *ApJ*, 443, 152
- Wright, E. L., et al. 1991, *ApJ*, 381, 200